Stem Cell Research & Therapy

REVIEW

Open Access

The interplay of cells, polymers, and vascularization in three-dimensional lung models and their applications in COVID-19 research and therapy

Toka A. Ahmed[1,3], Bassant Eldaly[1], Shadwa Eldosuky[1], Hoda Elkhenany[2], Azza M. El-Derby[1], Muhamed F. Elshazly[1] and Nagwa El-Badri[1*]

Abstract

Millions of people have been affected ever since the emergence of the corona virus disease of 2019 (COVID-19) outbreak, leading to an urgent need for antiviral drug and vaccine development. Current experimentation on traditional two-dimensional culture (2D) fails to accurately mimic the in vivo microenvironment for the disease, while in vivo animal model testing does not faithfully replicate human COVID-19 infection. Human-based three-dimensional (3D) cell culture models such as spheroids, organoids, and organ-on-a-chip present a promising solution to these challenges. In this report, we review the recent 3D in vitro lung models used in COVID-19 infection and drug screening studies and highlight the most common types of natural and synthetic polymers used to generate 3D lung models.

Keywords COVID-19, Lung organoid, Synthetic polymers, Lung spheroid, Natural polymers

Introduction

Developing a treatment for the novel coronavirus COVID-19 has faced multiple challenges in defining the pathogenesis, target cells, the mechanisms of initiation and progression of the disease, and drug testing [1]. Development of effective COVID-19 treatment requires comprehensive understanding of the pathology caused by the new virus. As the virus' primary target is the respiratory system and the lung tissue [2], there is a need for developing an in vitro 3D culture system that resembles the complexity of the in vivo conditions, has its own vascular support, and could be patient-specific.

Traditional 2D cultures are commonly used to study viral biology, drug discovery, and vaccine development. However, 2D culture systems do not resemble the biochemical microenvironment or the proper physiology of the human body [3]. Three-dimensional cell culture can serve as a better model for mimicking the internal microenvironment, leading to higher accuracy in the data of viral and antiviral compounds screening studies [4]. Data collected from research on scaffold-based or scaffold-free 3D culture models have shown superior accuracy and applicability to the in vivo models.

This was especially evident in studying diseases that lack a representative animal model such as brain and skin cancers [5, 6]. Moreover, 3D systems make inaccessible human tissue easier to model and investigate. For example, brain organoids were used to advance studies

*Correspondence:
Nagwa El-Badri
nelbadri@zewailcity.edu.eg
[1] Center of Excellence for Stem Cells and Regenerative Medicine (CESC), Zewail City of Science and Technology, October Gardens, 6th of October City, Giza 12582, Egypt
[2] Department of Surgery, Faculty of Veterinary Medicine, Alexandria University, Alexandria 22785, Egypt
[3] Egypt Center for Research and Regenerative Medicine (ECRRM), Cairo, Egypt

in developmental neurobiology and exploring brain disorders [7, 8]. In vivo studies using animal models are expensive, time-consuming, and heavily monitored in accordance with the three Rs principle, replacement, reduction, and refinement, of humane animal research [6, 9]. 3D models thus present a more relevant representation than 2D cultures and a more convenient system than in vivo models, facilitating routine experiments.

3D culture models present a valuable tool to study severe acute respiratory syndrome coronavirus 2 (SARS-CoV-2) mechanisms of infection replication and antiviral therapies. A multicellular spheroid is one of the 3D culture system methods in which cells are organized in spherical cellular aggregations [10]. In low attachment culture, spheroid formation is driven by the tendency of the cells to aggregate and self-assemble. This process is similar to what happens in nature during organogenesis [11]. 3D culture systems depend on factors that include the types of cells, the culture medium, specific growth factors, and scaffolds. In this review, we survey the components and factors that should be considered during generating lung spheroids as models for respiratory disease. These include the cell composition, matrix type, and vasculature system as well as the implementation of these models in COVID-19 studies.

History of lung spheroid generation

Airway epithelium provides one of the first defenses against inhaled toxic substances and airborne pathogens (e.g., corona viruses) [12, 13]. Creating a reliable human lung spheroid model is necessary for studying lung development and pathologies, as well as testing new drugs or therapeutic methods to relieve respiratory diseases. Spheroids are self-assembled 3D structures where cells aggregate upon their culture on non-adhesive surfaces [14]. The first lung model having a 3D structure was generated by Benali and collaborators in 1992. In this model, human primary epithelial respiratory cells isolated from nasal polyps and tracheal gland epithelial cells were cultured on collagen matrix [15]. Generation of spheroids entailed their culture on non-adhesive culture flasks/wells [16], on hydrogel matrices or scaffolds [17], and in bioreactors [18]. Other culture methods used to mimic the physiological microenvironment include the hanging drop method (HD) [19], spinner flask technique [10], microfluidic 3D cell culture [20], and liquid overlay [21]. The hanging drop method is considered one of the simplest methods to form lung spheroids. In this method, cells are seeded into a small drop that is later inverted so that the cells aggregate at the bottom of the drop forming spheroids [19]. In a study by Liu et al., A549 adenocarcinoma human alveolar basal epithelial cell line was cultured using the HD method to form an in vitro 3D lung model [22]. This model merged a HD culture system and an air exposure system that allowed for direct contact between the cells and volatilized air toxicants, and provided a promising air exposure system that could be used in inhalational drug delivery studies and environmental risk assessment [22]. In hydrogel systems, Delgado et al. reported that seeding the cells within the gel displayed different results in spheroid structures than those on the surface of the gel [23]. In microfluidic systems, microfluidic chips can be optimized for different culture conditions to enhance lung spheroids generation [24]. Zuchowska et al. used a microfluidic lab-on-a-chip system for lung spheroid generation to test the efficiency of photodynamic therapy (PDT) on A549 spheroids. The microchip was designed to allow for direct spectrofluorometric measurements on the formed spheroids by placing the microchip in a chip holder. The study showed that PDT was lethal to cancer spheroids [25]. Culture conditions also play a pivotal role in lung cell expansion and spheroid generation. For instance, supplementing the culture medium with epidermal growth factor (EGF) and retinoic acid was reported to be crucial for lung cell growth [26]. Hagiwara et al. showed that EGF was essential for inducing branch formation of the normal human bronchial epithelial cells (NHBEs) cultured in Matrigel, as well as enhancing their migration [27]. In other studies, Rho-associated protein kinase inhibitors (ROCKi) were reported to enhance the proliferation rate of primary human airway epithelial basal cells in 2D cultures [28, 29]. To better simulate the complexity of the physiological microenvironment in the formed spheroids, other cell types such as endothelial cells (ECs) and fibroblasts were integrated [26]. Butler et al. compared tracheosphere formation derived from basal cells in two different culture media. Mitotically inactivated fibroblasts (3T3-J2) were incubated either with a ROCKi known as Y-27632 (3T3 + Y) in serum-containing epithelial growth medium, or with bronchial epithelial growth medium (BEGM) only. The study showed that tracheospheres derived from BEGM-cultured cells were dependent on the cell passage number. Passage 4 BEGM cells produced smaller tracheospheres when compared to the first passage. On the other hand, development of tracheospheres derived from 3T3 + Y cultured basal cells were not influenced by passage number [29].

When compared to 2D culture models, 3D lung spheroid models were shown to be superior in anticancer drug testing [30]. For example, TTA-A2 anticancer drug tested on A549 cell line spheroid cultured in agarose-coated plates was found to have a potent anticancer effect when compared with monolayer culture [31]. Similar data were reported in virus infection models. A549 cell line was used to generate a lung spheroid model for

respiratory syncytial virus (RSV) infection using ultra-low-attachment plates. The model's efficiency was evident in effective demonstration of RSV infection key features such as mucin secretion [32]. In another recent study, lung alveolar spheroids using A549 cells embedded in Matrigel matrix were used to validate deep learning uncovered measurement of epithelial networks (DeepLUMEN) assay. A detection algorithm was successfully optimized to spot morphological changes in lung spheroids from bright-field images in response to different drug treatments and extracellular matrix (ECM) compositions [33]. Lung spheroids were also generated from A549 cells using rotating-wall vessel bioreactor to investigate the interaction between *Pseudomonas aeruginosa* and lung epithelial cells. In this model, *P. aeruginosa* was less effective in penetrating A549 spheroids than their monolayer counterpart and had higher levels of proinflammatory cytokines after infection, suggesting that the spheroid culture system showed more accuracy in the study of *P. aeruginosa* pathogenesis [34].

Generation of lung spheroids from type II alveolar epithelial cells (AEC2) has faced some challenges. Human-induced pluripotent stem cell-derived AEC2 were generated to overcome the difficulty of growing and maintaining human endogenous AEC2 in vitro [35]. Shiraishi et al. explored the possibility of culture expanding endogenous human AEC2 using a combination of ligands and inhibitors for crucial signaling pathways. These included Notch and fibroblast growth factor 7 (FGF7) ligands, glycogen synthase kinase 3 (GSK-3β), transforming growth factor beta (TGF-β), and bone morphogenetic protein 4 (BMP4) inhibitors. AEC2 cultured in Matrigel in transwell clear inserts successfully generated 3D spheroids [36]. Dinh et al. generated lung spheroids from whole lung tissue samples and transbronchial biopsy samples. Outgrown cells from cultured tissue explants were seeded onto ultra-low-attachment flasks generating lung spheroids, which contained a mixture of club cells, alveolar type 1 (AT1) cells, and alveolar type 2 AT2 cells together with $CD90^{+}$ and $CD105^{+}$ stromal-origin cells. The methodology adopted in this study could pave the way for cell-based therapies utilizing extracted lung stem cells for the treatment of lung diseases [37].

Another important type of cells used in the generation of multicellular lung spheroids is adult stem cells. Stem cell populations in the lung epithelium include basal cells [38], AEC2, pulmonary neuroendocrine cells (PNECs), and bronchioalveolar stem cells (BASCs). Basal cells spread throughout the airways and are capable of self-renewal and mucociliary differentiation into ciliated and secretory cells [38, 39]. AEC2 constitute the stem cell niche in the respiratory zone and can differentiate into alveolar epithelial type 1 (AEC1) [40]. PNECs are spread throughout the conducting airways and are capable of differentiating into ciliated cells and club cells [41]. BASCs are found between the conducting and respiratory zones border and can differentiate into AEC2 and Club cells [42, 43]. For example, Rock et al. generated 3D spheroids (bronchospheres) from primary basal cells expressing Trp-63 and nerve-growth factor receptor (NGFR). Basal cells cultured in Matrigel matrix proliferated and successfully produced bronchospheres containing a basal cell layer. A second layer of differentiated goblet and ciliated cells was also developed [38]. As mentioned, human pluripotent stem cells (hPSCs) including both embryonic stem cells and induced PSCs can be used in generating 3D airway models after step-by-step differentiation as previously reported [44–47]. However, these models generated from differentiated stem cells are composed of multiple cell types and are mostly referred to as "organoids" rather than spheroids.

Lung spheroids and COVID-19

SARS-CoV-2 is a positive single-stranded RNA liable for the serious COVID-19. SARS COV-2 binds to the enzymatic domain of the angiotensin-converting enzyme 2 (ACE2) receptor on the surface of various cell types, including alveolar cells, intestinal epithelial cells, ECs, kidney cells, neurons, and monocytes/macrophages [48]. The spike (S) protein, which is made up of two subunits, is responsible for coronavirus binding to host cell surface receptors and membrane fusion processes (S1 and S2). After the binding of S protein to ACE2 receptor, the intracellular protease transmembrane serine protease 2 (TMPRSS2) controls the cleavage and activation of S protein in SARS-CoV-2, resulting in unlocked, fusion-catalyzed forms on the cell surface. This promotes earlier viral body entry [49, 50]. Despite the valuable data generated from 2D cultures in early SARS-CoV-2 studies, using 2D models did not accurately represent the complexity and heterogeneity of the physiological in vivo microenvironment, resulting in inaccurate outcomes in drug screening [3]. 3D cultures represent a promising alternative model that accurately mimic the complexity of the physiology and microenvironment of the organ where the infection of SARS-CoV-2 naturally occurs [4]. Table 1 provides a summary of the studies that used 3D culture models, composed of organoids or spheroids to mimic the physiological environment of human organs in cases of SARS-CoV-2 infection (Table 1). Many of these models were shown to be superior to traditional culture for drug discovery. Lung organoid models used in SARS-CoV-2 research are based on the development of the distal airway, including AT2 cells, and express high levels

Table 1 Three-dimensional lung models used in COVID-19 studies

3D lung model	Cell composition	3D matrix/method	Application of the model	Key findings	References
Lung organoid	hPSCs	100% Matrigel	Screening compounds for SARS-CoV-2 inhibition	Susceptibility of (hPSC-LOs) specifically AT2s to SARS-CoV-2 infection Similar chemokine induction pattern to COVID-19 patients	[58]
Distal lung organoids	Alveolar epithelial type II (AT2) or $KRT5^+$ basal cells	Basement membrane extract II	Developing SARS-CoV-2 infection model	Successful infection of AT2, basal cells Identifying $SCGB1A1^+$ club cells as a target population No infection of ciliated cells	[59]
Alveolar spheroids	hAT2	Matrix-free model	Developing SARS-CoV-2 model	Rapid viral replication and high expression of proinflammatory and interferon-associated genes in hAT2 cells	[52]
Alveospheres	Human AT2 cells/ pneumocytes	Matrigel	Developing culture method for enhanced propagation and differentiation of alveospheres and test their validity for SARS-CoV-2 studies	40% of AT2s expressed ACE2 and about 80% were positive for TMPRSS2 activation of type II IFN pathway in AT2s Pre-treatment with IFNs shows prophylactic effectiveness in alveolospheres	[60]
(hBO)	Human bronchial epithelial cells	Matrigel—GFR basement membrane matrix	Establishing a proximal lung model for SARS-CoV-2 drug screening	High expression of ACE2 and TMPRSS2 after SARS-CoV-2 infection of hBO Increased levels of cytotoxicity, intracellular viral genome, progeny virus, and moderate elevation in type I interferon signal	[61]
Lung organoid	Human lung airway epithelial cells, basal stem cells, and pulmonary Microvascular ECs	Microfluidics Organ-on-a-chip + ALI	Developing organ-on-a-chip model to study influenza and SARS-CoV-2 viruses	Differentiated airway cells at ALI on-chip showed large increases in protein and mRNA expression levels of the SARS-CoV-2 receptors (ACE + TMPRSS) Two out of seven clinically approved drugs showed significant entry inhibition of the pseudotyped SARS-CoV-2 virus	[63]
hAWOs + hALOs	(hESCs)	Matrigel	Developing a model for SARS-CoV-2 infection and drug testing	All viral infected cells expressed ACE2 but not all ACE2-expressing cells were infected Ubiquitous expression of TMPRSS2 in both hAWOs and hALOs Club cells were identified as new target cells of SARS-CoV-2 Significant down-regulation in metabolic processes especially lipid metabolism after infection	[66]

Table 1 (continued)

3D lung model	Cell composition	3D matrix/method	Application of the model	Key findings	References
Complete lung organoid	Lung cells obtained from biopsies + hiPSC-derived alveolar type-II (AT2) pneumocytes	Cold Matrigel	Producing a scalable and cost-effective 3D complete lung model	Infected ALO monolayers had the best recapitulation to transcriptomic signatures in COVID-19 patients Distal alveolar differentiation (AT2 → AT1) 3D-to-2D conversion virtually abolished the AT2 signatures, showing prominent emergence of AT1 signatures	[64]
Alveolar organoids	Primary epithelial cells isolated from normal human distal lung tissue	Cold Matrigel	Establishing 3D model to study the response of proximal and distal lung epithelium to SARS-CoV-2 infection	Transcript profiles of infected organoids showed high levels of SARS-CoV-2 viral RNA High levels of cytokines and antiviral response genes No significant change in the expression of AT2 cell marker, as ACE2 and TMPRSS2 was observed	[67]
Lung organoids	hESC	Matrigel	Investigating the high prevalence of severe complications of SARS-CoV-2 in men and relative immunity in children	Androgen increased the expression of viral receptors and SARS-CoV-2 infectivity Screened antiandrogenic drugs decreased SARS-CoV-2 infectivity	[68]

of ACE2 and TMPRSS2 which are required to study the viral infection and pathogenesis [51–53].

SARS-CoV-2 does not only cause lung damage, but also affect several organs such as the liver [54], the kidneys [55], the cardiovascular system [56], and others that express ACE2. However, the highest expression of ACE2 occurs in human type II alveolar cells in the lungs, which is the most affected organ in Covid-19 patients [57]. Generation of lung organoids has been recently pursued as one of the most relevant models for SARS-CoV-2 studies. For instance, Han et al. succeeded in developing a lung organoid model from hPSCs (hPSC-LOs) using 100% Matrigel dome matrix. HPSC-LOs, specifically the alveolar type-II-like cells, were susceptible to SARS-CoV-2 infection and induced chemokines in a pattern that was similar to that of COVID-19 patients [58]. On the other hand, Salahudeen et al. used basement membrane extract II (Trevigen) matrix to develop a model of distal lung organoids derived from human AEC2, or $KRT5^{+}$ basal cells. To facilitate the viral access to the ACE2-expressing luminal cells, the researchers used an apical suspension culture to allow the virus easy access to the intact apical surface and to reach the site of infection. AT2 cells, basal cells, and $SCGB1A1^{+}$ club cells were identified as a target for viral infection, while no infection was observed in ciliated cells. The researchers concluded that alternative culture conditions may be required [59].

Alveolar spheroids represent another model for SARS-CoV-2 studies. Youk et al. established a matrix-free model of 3D human alveolar stem cells (hAT2) derived from primary human lung tissue using chemically defined culture conditions. The aim of this model was to stimulate self-organization of single hAT2 cells into alveolar-like 3D structures. Rapid viral replication was achieved, and high expression of proinflammatory and interferon-associated genes in hAT2 cells was observed, demonstrating a robust endogenous innate immune response [52]. Similarly, Katsura et al. developed a culture system for enhanced propagation and differentiation of alveospheres, derived from human AT2 cells/ pneumocytes. Culture conditions were optimized using murine and human AT2s on Matrigel-coated plates in a serum-free feeder-free medium. Results showed the activation of type-II IFN pathway in AT2 cells. Furthermore, pretreatment with interferons (IFNs) showed prophylactic effectiveness of the alveolospheres [60].

To establish a proximal lung model, Suzuki et al. used cryopreserved human bronchial epithelial cells to develop human bronchial organoids (hBO) on Matrigel growth factor reduced (GFR) basement membrane matrix. The study showed high expression of ACE2 and TMPRSS2 after infection of hBO with SARS-CoV-2. In addition, increased cytotoxicity, intracellular viral genome, progeny virus, and moderate elevation in type I interferon signal were observed [61].

Using microfluidics technology [62], Si et al. used air–liquid interface (ALI) to generate 3D lung models to mimic surfactant-dependent alveolar homeostasis [63]. Human lung airway epithelial basal stem cells and pulmonary microvascular ECs were tested on pseudotyped SARS-CoV-2 virus on a microchip. Differentiated airway cells at the ALI showed large increases in protein and mRNA expression levels of both SARS-CoV-2 receptors ACE2 and TMPRSS. Despite these interesting findings, only two out of seven clinically approved drugs, amodiaquine and toremifene, showed significant entry inhibition of the pseudotyped SARS-CoV-2 virus [63].

Using the same ALI method, Tindle et al. used cold Matrigel matrix to establish adult lung organoids (ALOs) complete with both proximal airway and distal alveolar epithelia [64]. This method showed both cost-effectiveness and scalable 3D complete lung model. When comparing the infection of ALOs with human-induced pluripotent stem cells (hiPSCs)-derived AT2 pneumocytes, the first showed the best recapitulation to transcriptomic signatures in COVID-19 patients, whereas distal alveolar differentiation ($AT2 \rightarrow AT1$) was crucial for producing a profound host immune response [64].

To enhance the generation of 3D organoids, Pei et al. developed two 3D models of human airway organoids (hAWOs) and alveolar organoids (hALOs). Both organoids were derived from human embryonic stem cells (hESCs) using Matrigel along with defined growth factors. All viral infected cells expressed ACE2 but not all ACE2-expressing cells were infected. TMPRSS2 was expressed ubiquitously in both the hAWOs and hALOs, in contrast to the restricted expression pattern of ACE2. In addition to club cells, a type of bronchial epithelial cells was identified as new target cells of SARS-CoV-2. Furthermore, significant down-regulation in metabolic processes especially lipid metabolism after SARS-CoV-2 infection was reported [65, 66].

Mulay et al. used an ALI culture system on Matrigel to create a primary human lung epithelial 3D lung model to study the response of proximal and distal lung epithelium to SARS-CoV-2 infection. Transcript profiles of infected organoids showed high levels of viral RNA, indicating successful replication and gene transcription in the produced organoids, in addition to high levels of cytokines and antiviral response genes. However, no significant change in the expression of AT2 cell markers such as ACE2 and TMPRSS2 was observed [67].

To investigate the high prevalence of severe complications of SARS-CoV-2 in men and relative immunity in children, Samuel et al. used lung organoids derived from hESCs using Matrigel matrix. Androgen was shown to

increase the expression of viral receptors, leading to increased SARS-CoV-2 infectivity, and antiandrogenic drugs were shown to decrease the infectivity [68].

Vascularization of 3D models

The vascular network formation is the result of the orchestration between the vasculogenesis and angiogenesis [69]. Angiogenesis is the formation of new blood vessels from existing ones; it comprises ECs proliferation, migration, polarization, sprouting, maturation, and stabilization to end with new functional blood vessel [70, 71]. On the other hand, vasculogenesis is the de novo formation of the blood vessels through the differentiation of mesodermal-derived hemangioblasts. Angioblasts are the ECs precursors that develop into intraembryonic vasculature of the neural tube, limbs, and organ-specific vascular plexus [72, 73]. In the early stages of the embryonic development, embryonic stem cells (ESCs) give rise to three germ layers, "ectoderm, endoderm, and mesoderm." Both vascular ECs and hematopoietic cells have mesodermal origin [74]. Vasculogenesis in the embryo is followed by angiogenesis which in turn comprises endothelial cell division and sprouting migration, controlled by the vascular endothelial growth factor (VEGF)-Notch pathway [75, 76]. The newly formed blood vessels become lined internally with stalk cells, followed by specialization into arteries and veins, under the influence of several internal and external signals including ephrinB2-EphB4, VEGF, Notch, delta-like ligand 4 (Dll4), and Chicken Ovalbumin Upstream Promoter Transcription Factor II [77–79]. Sporulation is followed by elongation and maturation of the newly formed blood vessels, aided by the contractile mural cells [80]. Mural cells play important role in angiogenesis via matrix metalloproteinase (MMP) secretion [81], basement membrane formation, and ECs permeability regulation [82, 83]. The absence of vascularization in the engineered tissues leads to cell starvation and hypoxia which in turn ceases the cell growth and may lead to alteration in the cell phenotype and loss of functionality, and eventually cell death [84, 85]. The absence of vascularization also has a significant role in hindering the tissue's regenerative capacity [86, 87]. Vascularization could be introduced to the engineered spheroids or organoids to mimic the original physiological or pathological state. Despite the plethora of organoid models for drug screening and disease modeling, most of these are not complete due to the absence of vasculature [88]. The pre-vascularized organoid is an excellent platform to study the role of angiogenesis in organogenesis and regeneration [89, 90]. Vascularization can be introduced to the organoid either by the induction of angiogenesis or incorporation of microvasculature network [91]. ECs are the most common cells to be incorporated for vascularization, due to their inherent angiogenic properties and their ability for self-assembly into a vascular network that integrates with host vasculature [92]. However, the limited proliferation potential of the terminally differentiated cells and the absence of the supporting mural cells represent a technical challenge [93, 94]. One of the important vascularization approaches is ECs spheroid culture which was first developed to mimic the in vivo cell–cell interaction [95]. Spheroid culture suffers the development of a hypoxic core that results from cell aggregation and the significant decrease in oxygen diffusion. The hypoxic core thus stimulates the expression of hypoxia-inducible factor-1 (HIF-1) and its downstream target VEGF which in turn binds to VEGF receptor and modulates the angiogenesis through extracellular regulating kinase 1/2 (ERK-1/2) and mitogen-activated protein kinase (MEK-1/2) pathways. These events shift the environment to a proangiogenic one that better stimulates physiological angiogenesis. However, vascular network should contain other components than the endothelial tube, such as smooth muscle cells, basal lamina and pericytes (PCs) [96]. Indeed, pre-vascularized, spheroids that comprise both vascular cells such as human umbilical vein endothelial cells (HUVEC) and other types of cells showed an obvious ability to mimic the complexity of tissue microenvironment in cases of cardiac tissue [97] and hepatic tissue [98]. Moreover, HUVEC were reported to be used in combination with human umbilical artery smooth muscle cells (HUASC) to generate a vascularized porcine intestinal model [99]. In another study, a spheroid model comprising HUVEC and HUASC showed a decline in the level of platelet-derived growth factor beta (PDGF-B) compared with HUVEC alone. This may be attributed to the potential of the spheroid model to mimic the in vivo environment, where PDGF-B disappears after capillary maturation [100]. Cardiac spheres that comprise both HUVEC and cardiomyocytes displayed capillary-like network formation that contributed to the viability and maintenance of the functionality, phenotype, and longevity of the cardiomyocytes [101]. Interestingly, macrophages were reported as another supporting type of cells that can contribute to remodeling of the microvasculature during angiogenesis via their growth factor-rich secretome, phagocytosis, trafficking, and proliferation behavior. Dohle et al. reported that co-culture of ECs and primary osteoblasts exhibited an increasing number of capillary-like structures when exposed to macrophages compared to controls. This could be attributed to the elevated levels of VEGF in the co-culture condition [102]. Walser et al. demonstrated that co-culture of spheroids of human osteoblasts and dermal endothelial cell (DECs) successfully formed microvascular-like capillaries that interconnected with host vasculature when transplanted

in vivo. Human dermal fibroblasts (HDFs) co-culture exerted no significant effect on the vascularization level in that model [103]. Mesodermal progenitor cells (MPCs) derived from human iPSCs have been used to generate vascularized organoids overcoming the limitations of the ESCs. Wörsdörfer and colleagues generated vascularized neural and tumor organoids by co-culture of MPCs with the neural spheres and tumor cells respectively. The in vitro formed blood vessels displayed the potential to connect the blood vessels in the chicken chorion allantois membrane (CAM) [88]. In contrast to using terminally differentiated ECs, this model showed hierarchic organization of the blood vessels and assembly of mural cells into the vessel wall. Moreover, high plasticity and maturation in the endothelial network of the growing organoids has been reported, including responsiveness to the proangiogenic and anti-angiogenic factors.

Endothelial progenitor cells (EPCs), first reported by Asahara et al. as a circulating $CD34^+$ population in the peripheral blood, are considered an important cell source for vascularization. EPCs were shown to integrate with the blood vessels and restore neovascularization after injection into the ischemic hind limb of a mouse model [104]. Loibl et al. reported that co-culture of EPCs and mesenchymal stromal cells led to differentiation of the latter into PC-like cells expressing the PC markers Neuron-glial antigen 2 (NG2) and alpha smooth muscle actin (α-SMA) [105]. Moreover, using polyurethane scaffold, Duttenhoefer et al. successfully developed a vascularized construct enriched with $CD34^+$ and $CD133^+$ EPCs and mesenchymal stromal cells (MSCs) [106].

MSCs are another important cell source for vascularization of engineered tissues, by means of differentiating into the endothelial-like cell under the influence of a predefined differentiation cocktail. Wang et al. reported that treatment of bone marrow-derived MSCs with VEGF and basic fibroblast growth factor (bFGF) for one week induced the expression of EC markers [107]. Au et al. reported that co-culture of bone marrow-derived MSCs and HUVECs induced the differentiation in the former into functioning pre-vesicular cell [108]. The same results were reported by Laranjeira et al. who showed that co-culture of human DECs and MSCs caused the latter to express high levels of collagen 1 and VEGF165 [109], and elevated the levels of their angiogenic secretome [110]. Stenderup and colleagues demonstrated that when ECs were co-cultured with MSCs, each cell type migrated toward its specific niche and formed separate aggregates that contacted sporadically. The culture medium was found to greatly influence the differentiation potential and proliferation of the co-cultured MSCs toward ECs [111, 112]. Co-cultured MSCs with ECs in fibronectin-containing collagen contributed to the vasculogenesis of the engineered construct [86]. In another study by Deegan and colleagues, dynamic culture conditions had a positive effect on cellular functions, arrangement, and interaction between the HUVEC and MSCs [113]. Using a suitable cocktail of growth factors enhanced cell differentiation in generating vascularize organoids. A study by Morita et al. showed that human fibroblasts had the potential to be converted into functional ECs using erythroblast transformation-specific transcription factor 2 (ETV2) [114]. ETV2 contributed a significant role in generating endothelial lineages from HDFs with more than 90% efficiency through delivery of modified mRNA encoding ETV2 [115]. More recently, Cakir et al. have incorporated 20% of doxycycline-inducible ETV2 gene-transduced iPSCs to the 3D aggregates during their initial formation. Their data showed successful formation of vascular structures within the cerebral organoids [116]. Although many studies showed that vascularization is an important factor to generate biomimetic 3D models of numerous tissues, only few studies reported the generation of vascularized lung spheroids or organoids. Further studies to enhance the generation of vascularized 3D lung models are needed to accelerate their application in drug testing and molecular studies for COVID-19 research.

Polymers for 3D cell culture and spheroid formation

Scaffolds are considered the basis of tissue engineering and essential for organ reconstruction [117]. The generation of well-patterned and functional organoids depends on the ECM structure and mechanical properties of the biomaterial used [118]. Natural and synthetic biomaterials have been utilized reliably to generate organoids with physicochemical and biomechanical properties that mimic the native tissues and reliable for disease modeling and drug discovery. Natural biomaterials represented in protein and polysaccharide polymers have been investigated in various tissue engineering applications (Table 2, Fig. 1). Herein, we review the properties of the biomaterial as a suitable matrix for lung tissue regeneration.

Natural biomaterials

Protein polymers

Collagen

Collagen is a natural polymer and one constituent of the lung ECM. Collagen forms about 15% of the dry weight of human lung [119], and can be identified in alveolar interstitium, and bronchi and blood vessels in several types (Type I, III, IV, V, and VI) [119, 120]. Collagen possess high tensile strength by which it can control parenchymal expansion and prevent airway collapse [121]. Hamilton, et al. [122] reported that collagen type I scaffold protected tracheospheres generated from airway lung basal cells and fibroblasts, and enhanced

Table 2 Properties of natural and synthetic polymers exploited for culture of 3D cellular spheroids

Type	Name	Features to support spheroid culture	References
Protein polymers	Collagen	Biocompatibility No cytotoxicity Good tensile strength Low immunogenicity Lack mechanical strength and structural stability upon hydration	[122, 215]
	Silk fibroin	Adhesive properties High mechanical strength Biocompatibility	[129, 131]
	Fibrin	High availability and biocompatibility viscoelastic properties Low cost	[135, 216]
	Matrigel	Liquid at temperatures below 8 °C Solid at temperatures above 8 °C Biocompatibility Mechanical properties Heterogenic variability from batch to batch	[217–219]
Polysaccharide polymers	Glycosaminoglycans	Biocompatibility Maintain viscoelasticity of tissue	[164]
	Hyaluronic acid	Hydrophilicity Biocompatibility Limited immunogenicity	[169, 220]
	Chitosan		
	Shrimp chitosan	Elongated pores Low water absorption properties and degradation rate Enhanced cell attachment	[172, 179, 221, 222]
	Fungal chitosan	Polygonal pores High water absorption and degradation properties Enhanced cell attachment and proliferation	
Synthetic polymers	PNIPAm	Thermoresponsive properties Biocompatibility	[3, 20, 202, 204]
	PDMS	Hydrophobicity Biocompatibility High oxygen permeability Simple preparation techniques	[20, 210, 211]
	PCL	Rheological and viscoelastic properties (i.e., solubility and low boiling point) accommodating different fabrication techniques Low cost	[2, 19, 217, 218]

vascularization upon implantation into decellularized tracheal scaffold. In addition to being biocompatible, collagen was found to be non-cytotoxic, reduced the fibrinogenic phenotype of bone marrow mesenchymal stem cells (BM-MSCs), and enhanced their regenerative capacities [123]. Collagen type I loaded with BM-MSCs generated cartilage-like tissue similar to native ECM, both mechanically and morphologically [124]. Collagen has been shown to trigger MMP-dependent directional migration of stromal cells from endometrial spheroids [125]. Type I collagen mixed with glycosaminoglycan (GAG) was found to maximize its potential to form matrix for better alveolar regeneration [126]. The alveolar-like structures generated by this scaffold had the ability to contract, as confirmed by positive expression of α-smooth muscle actin. Type I collagen also provided a suitable matrix for generation of multicellular tumor spheroids to study lung cancer [127].

Silk fibroin

Silk fibroin (SF) is a natural protein polymer derived from *Bombyx mori cocoons*. SF has been classified as an excellent biomaterial for tissue regeneration [128]. One of its components is sericin, which was classified as an adhesive protein [129], characterized by a controllable degradation rate [130]. Silk fibers showed high mechanical strength in which 7.25 MPa estimated the ultimate tensile strength. These properties prompted its application in trachea tissue regeneration [131]. Three-dimensional SF scaffold loaded with tracheobronchial epithelial cells enhanced epithelial regeneration with less fibrosis in experiments to reconstruct a tracheal defect in rabbit [131]. Electrospun scaffold of SF could also provide ECM that is architecturally and morphologically similar to native tissue [132]. Human umbilical cord MSCs (UC-MSCs)-loaded SF scaffold enhanced cell proliferation, reepithelization, vasculogenesis and most importantly

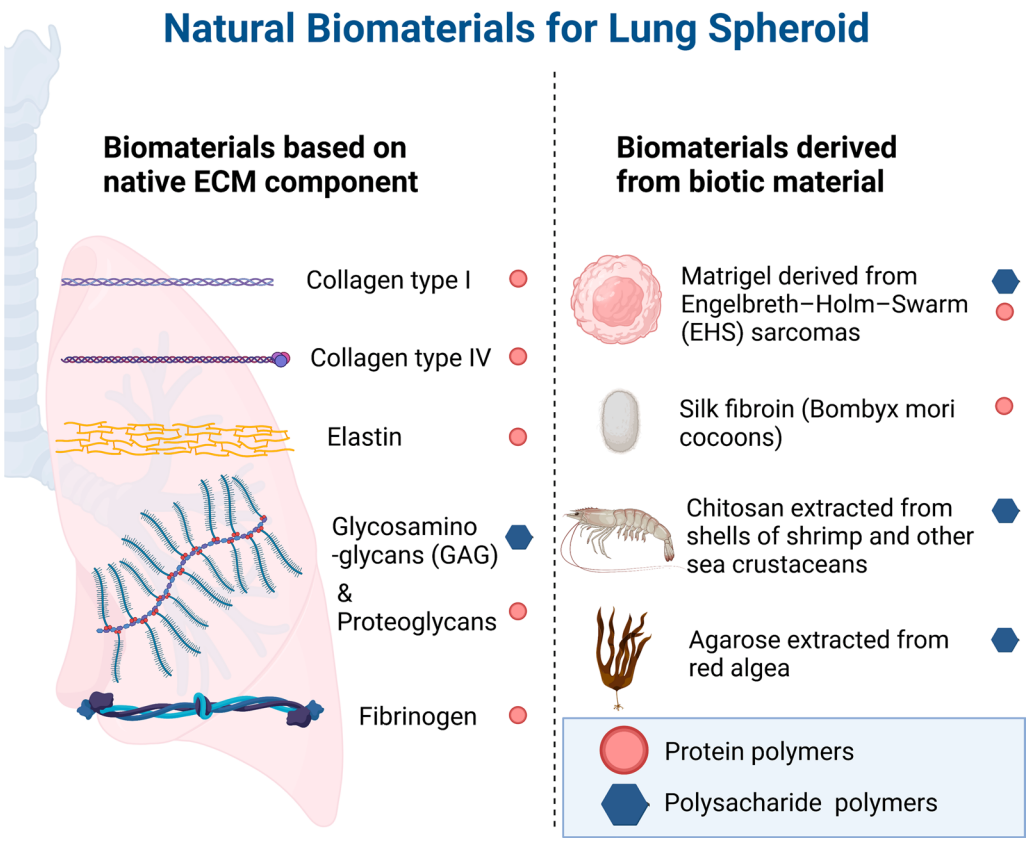

Fig. 1 Schematic diagram showing the natural biomaterials for lung spheroid generation. This figure was created with BioRender.com

reduced scar formation in skin regeneration [132]. SF scaffold loaded with human adipose stem cells (ASCs) also have shown strong angiogenic potential using chorioallantoic membrane model [133].

Fibrin

Fibrin biopolymer formed after activation of fibrinogen by thrombin plays role in blood clotting, inflammatory response, and wound healing [134]. The availability, porosity, biocompatibility and low cost of fibrin hydrogel present it as an acceptable scaffold for tissue engineering [135]. Fibrin-based scaffolds are characterized by their ability to maintain their architecture, while lacking contractile properties. These properties supported their applications in particular tissue scaffolds thanks to their high reproducibility and integrity compared to collagen-based matrix [136, 137]. For example, cross-linking fibrin hydrogel with alginate–chitosan composite enhanced the cell differentiation and generation of self-organized liver organoids [138]. Combining fibrin with polypropylene fumarate enhanced the vascularization of neobone tissue [139]. In combination with laminin, fibrin scaffolds have been demonstrated to provide physical support for organoid formation and long-term expansion [140]. Moreover, fibrin hydrogel mixed with other materials, such as polyethylene glycol (PEG) was used to tailor a 3D lung adenocarcinoma model [141], while a scaffold of fibrin and collagen microfibers was successfully used to investigate the vascular invasion of cancer [142]. In order to modulate the poor mechanical properties of fibrin, agarose has been used to increase its stiffness [143].

Matrigel

Matrigel is a hydrogel extracted from murine Engelbreth–Holm–Swarm sarcomas [144]. Matrigel consists of a diverse mixture of ECM proteins (laminin, collagen IV, and enactin), proteoglycan, and growth factors (including bFGF, EGF, insulin-like growth factor-1 (IGF-1), TGF-β, PDGF, and NGF) [145–147]. The high versatility of Matrigel to enhance 3D culture has been reported in different studies. For instance, Matrigel was used for culturing iPSCs in 3D culture to investigate the endochondral pathway [148], cerebral organoid formation [149], liver [150, 151], kidney [152], and intestinal crypt organoid [153]. However, some drawbacks have been reported including batch-to-batch variability and hard to determine factors that contributed to the regeneration due to composition complexity [154, 155]. Using Matrigel

in microfluidic system has provided an optimal environment to enhance cell migration at low concentration, but not at high concentration, and this was attributed to excessive cellular attachment [156]. It is worth mentioning that Matrigel has been used intensively in spheroid generation. Matrigel was the matrix of choice to study the complex differentiation process of iPSCs into ventral–anterior foregut spheroids and ultimately generation of lung organoids [157]. Human lung spheroids generated on Matrigel were used to investigate the lung's regenerative potential of pulmonary fibrosis in rodents [158]. In this study, it has been demonstrated that lung spheroid cells (LSCs) encapsulated into Matrigel could successfully differentiate into alveolar-like cells and generate alveoli-like structures that displayed positive aquaporin-5 (lung epithelial cell marker) staining. Matrigel has been successfully used to form primary lung tumor spheroids for testing antitumor drugs and understanding the tumor's pathophysiology [159–161].

Polysaccharide polymers

Glycosaminoglycans (GAGs)

GAGs are long, linear, and heterogeneous polysaccharides located at the alveolar interstitium, sub-epithelial tissue, and bronchial wall [162]. GAGs play an important role in the lung viscoelasticity [163]. Recently, it has been demonstrated that losing GAGs during lung decellularization had negative impact on cell attachment and growth, requiring replating the GAGs for better tissue regeneration [164]. However, combination of GAGs with collagen type I showed effective alveolar regeneration [126]. It has been reported that GAGs were involved in RSV infection [165]. Interestingly not all the GAGs had contribution to viral infection but only GAGs containing iduronic acid (like heparan sulfate and chondroitin sulfate B). Treating cells with protamine sulfate or GAG-destroying enzyme was shown to reduce viral infection [165].

In another study, chondroitin sulfate, a major population of GAGs, enhanced Japanese encephalitis viral replication in a neural cell line and the brain [166]. GAGs-related scaffolds may be used for SARS-CoV-2 disease modeling in vitro. We have recently reported that SARS-CoV-2 spike glycoprotein may interact with GAGs of the host cell surface as a mechanism to facilitate its entry to the host cell [167].

Hyaluronic acid

Hyaluronic acid (HA) is non-sulfated glycosaminoglycan that resides in all native tissue ECM and body fluids [168]. HA has shown a potential effect to stimulate cell proliferation, migration and attachment by interaction with CD44, receptor for hyaluronan-mediated motility (RHAMM), and intercellular adhesion molecule 1 (ICAM-1) receptors [169]. HA was also found to promote angiogenesis through RHAMM-transforming growth factor beta receptor-1 (TGFβRI) signaling pathway [170]. Interestingly, HA has shown a protective and therapeutic effect on lung tissue and alleviation of the toxic effect of bacterial pneumonia in an ex vivo model of lung injury [171]. On the other hand, HA possesses poor mechanical properties, which were overcome by cross-linking using chemicals [172], for example, mixing with collagen improved HA mechanical strength [173] It has been demonstrated that HA significantly increased stemness as confirmed by upregulation of NANOG, octamer-binding transcription factor 3/4 (OCT3/4), sex-determining region Y HMG-box 2 (SOX-2), and stage-specific embryonic antigen 3 (SSEA-3) gene expression and cell survival of ASCs compared to monolayer cultures [174]. In cosmetic applications, the viscoelastic properties of HA hydrogel supported its application in augmentation therapy for wrinkles [175]. Injection of human MSC spheroids encapsulated in HA hydrogel was effective in the regeneration of the fibrotic esophagus [176]. Moreover, hyaluronan–chitosan (HA–CS) biomaterial was used to generate a 3D lung tumor spheroid to investigate the cross talk of cancer cells and MSCs. Co-culture of MSCs and cancer cells on HA–CS was found to generate tumor spheroid in which MSCs aggregate in the spheroid center; however, the cancer cells aligned at the outer surface known as core–shell structure. The size of the spheroid was reported to correlate to the initial seeding cell number. Moreover, HA–CS scaffold was reported to increase cancer cells stemness, migration, and tumorgenicity [177].

Chitosan

Chitosan is a natural polysaccharide produced by deacetylation of chitin, derived from shells of shrimp and other crustaceans [178]. Chitosan extracted from *Gongronella butleri* fungi was reported to have superior biological and mechanical properties to shrimp chitosan [179]. In order to produce 3D porous scaffold, thermally induced phase separation (TIPS) technique are used to produce pore sizes that range from 1 to 250 μm depending on temperature and water content [180]. Increasing the porosity of chitosan was found to lead to increasing the surface area and decrease the scaffold elasticity; hence, integration with other polymers such as collagen was recommended to maintain the elasticity [181]. One of the chitosan disadvantages is low mechanical resistance and stiffness [181]. This can be optimized by cross-linking with other materials such as polyethylene glycol and starch [182]. Adding chitosan to collagen scaffold for skin regeneration was shown to enhance the biocompatibility

and biostability of the scaffold [181]. This combination was successfully used to generate 3D lung model to investigate influenza A infection [183]. In this study, collagen–chitosan 3D scaffold was shown to enhance the viability of the primary human small airway epithelial cells (HSAECs), and preserve the morphological characteristics of the native lower airway. 3D cultured HSAECs could successfully mimic the same in vivo airway epithelium characteristics as confirmed by aquaporin-5 and cytokeratin-14 expression [183].

Synthetic polymers

Synthetic polymers have been extensively used as supporting matrices for 3D culture of cellular spheroids for drug delivery and screening [184]. They offer several advantages over natural polymers thanks to their highly tunable properties that facilitate altering and optimizing experimental parameters to mimic the mechanical properties of various tissues in the in vivo environment [185]. However, since synthetic polymers are usually biologically inert, functionalization with cell adhesion peptide domains (e.g., arginylglycylaspartic acid (RGD)) is essential to promote cell adhesion and spheroid formation [186]. The tunable mechanical properties of synthetic polymers, depending on fabrication conditions, cross-linking, and copolymerization with natural and synthetic agents, allow for their exploitation in different biological applications. PEG is a hydrophilic polymer used frequently for the preparation of hydrogels. It exhibits relatively good mechanical properties. In addition to non-toxicity, PEG does not elicit an immune response, which makes it highly biocompatible and suitable for many biomedical applications. The properties of PEG are generally tunable with different fabrication methods including chemical and physical polymer cross-linking [187–189].

As a synthetic polymer, it lacks the biological moieties necessary for cellular activity, which makes it more suitable for ECM components during hydrogel preparation. Hybrid hydrogels incorporating gelatin within the photo-cross-linked PEG network improved cell adhesion and mechanical properties [188]. Moreover, the mechanical properties of PEG can be altered to match tissue stiffness that influences cell behavior. Through introducing a soluble allyl-presenting monomer to PEG–diacrylate hydrogel precursor solution before cross-linking, it was possible to reduce the stiffness within soft tissue regime (e.g., neural tissue) from 5.1 ± 0.48 kPa to 0.32 ± 0.09 kPa which demonstrates the potential of the compliant hydrogel system for examining the cell behavior in soft tissues [190]. PEG-based hydrogels were fine-tuned for lung spheroid generation. For instance, Gill et al. used a PEG hydrogel functionalized with two different bioactive peptides and mixed with murine lung adenocarcinoma cell line 344SQ exhibiting an expression behavior similar to human non-small cell lung adenocarcinoma. Arginine–glycine–aspartate–serine peptide (RGDS) was used for cell adhesion, while a MMP-sensitive peptide, GGGPQGIWGQGK (PQ), was used as a cell-degradable hydrogel backbone that can be cleaved by matrix metalloproteinase-2 (MMP-2) and matrix metalloproteinase-9 (MMP-9). Matrix stiffness was optimized by varying percentages of PEG in the matrix. This system successfully generated lumenized epithelial spheres similar to those observed in Matrigel culture. These experiments provided key evidence for the built-in differentiation capacity of cancer cells independent of matrix components. Most importantly, this study provided a reliable and modifiable tool to investigate the influence of ECM on tumor behavior by integrating other bioactive peptides and ECM ligands in the hydrogel system [191]. In another study by Roudsari and colleagues, the same PEG-based hydrogel system was modified by creating a dual layer hydrogel system where lung cancer cells (344SQ) are localized in one layer and HUVECin the other one. This study reported the development of a lung tumor angiogenesis model that could be used to investigate the interactions between vascular and cancer cells as well as the influence of vascularization on tumor progression [192].

Poly(N-isopropylacrylamide) (PNIPAm)

Poly-N-isopropylacrylamide (PNIPAm) is a smart thermoresponsive polymer used extensively in cell culture applications. Mediated PNIPAm substrates provide suitable conditions for cell adhesion and growth under physiological conditions. Additionally, the thermoresponsive properties of PNIPAm as a hydrophilic compound that becomes swollen at temperatures below 35 °C, and a hydrophobic one that shrinks at temperatures above 35 °C, allow efficient cell isolation. This can be achieved through altering surface hydrophobicity by means of changing temperature without the need for trypsin or other chemical agents [193–195]. Microgel particle size in the PNIPAm hydrogel was optimized and used for multicellular spheroid generation. This achieved reduced cellular uptake and improved physical properties (i.e., reduced shrinkage) [196, 197]. The biocompatibility of PNIPAm was validated by Capella and colleagues, who reported that PNIPAm hydrogel exhibited good biocompatibility, favorable cell attachment, and non-cytotoxic effect on A549 cell lines. These favorable biocompatible effects proved effectiveness in lung spheroids generation without detectable DNA damage [198]. In another line of research, PNIPAm-based hydrogel was also used for drug screening on human lung fibroblast (HLF) spheroids

[195], and formation of ASCs spheroids [199]. Dhamecha et al. reported the use of PNIPAm-based hydrogel microwell array (PHMA) for the high-throughput generation of spheroids using different cell lines including HLF and A549. Thanks to the thermoresponsive property of PNIPAm, tumor spheroids aggregated and formed at 37 °C and were readily isolated at room temperature. The matrix had suitable stiffness for spheroid culture and the formed wells were spherical and of uniform diameter throughout the PHMA, supporting the generation of uniform sized spheroids. Owing to the variabilities between cell–cell adhesion characteristics of each cell line, differences in spheroids morphology were observed. HLF generated spherical and compact spheroids while A549 displayed a more irregular morphology and took a longer time to be formed [195]. Results indicated the potential of PNIPAm-based hydrogel for reproducible, high-throughput culture of airway cells in a rapid, and cost-effective way [195, 199, 200].

Polydimethylsiloxane (PDMS)

Due to its strong hydrophobicity, PDMS-based compounds have been used for non-adherent cell culture. In addition to excellent biocompatibility, PDMS suits perfusion culture applications as it facilitates high oxygen permeability, which significantly enhances cellular growth and prevents hypoxia-induced necrosis, and the consequent formation of necrotic cores in 3D spheroids [201, 202]. PDMS was widely used in the development of microfluidic culture devices, which enables low cost, high-throughput culture of 3D spheroids, and efficient drug screening [203]. It was possible to fabricate tunable PDMS elastomeric wells using a one-step spontaneous interfacial reaction between aqueous droplets on liquid polydimethylsiloxane. This allowed easy and adjustable optimization of spheroid size leading to highly efficient co-culture of tumor cells and fibroblasts to replicate the in vivo complex microenvironment of cancer tissue [204]. PDMS plates developed using computer-aided design and manufacturing software showed great promise for mass production of spheroids and enhanced capacity for clinical applications. Furthermore, the fabricated plates enabled rapid formation of MSC spheroids within 24 h maintaining cell viability [205]. PDMS is a transparent, oxygen-permeable, and hydrophobic polymer that is widely used in microfluidic devices. Together with its simple preparation techniques, different surface modifications may be introduced to enhance surface hydrophobicity and facile spheroid release [20]. For SARS-CoV-2 applications, PDMS microfluidic devices showed promising results in forming 3D lung organoids that can be used to study the virus. For instance, Roy et al. proposed a new smart multichannel 3D cell culture microfluidic device using PDMS and other diverse polymeric porous/semipermeable membranes that can be implemented to form 3D lung organoids to study the pathogenesis of SARS-CoV-2 [206]. Similarly, Swank et al. developed a high-throughput microfluidic nanoimmunoassay (NIA) anti-SARS-CoV-2 antibody detection in serum or ultra-low-volume blood samples. Based on the analysis of 289 human serum samples, this method achieved a specificity of 100% and a sensitivity of 98% [207]. This device can further be used in current or future studies of serological or biomarker analysis of SARS-CoV-2.

Poly-ϵ caprolactone (PCL)

PCL is considered one of the easiest materials to accommodate in various types and shapes of scaffolds using different fabrication technologies. The synthetic polymer exhibits rheological and viscoelastic properties suitable for many fabrication techniques, such as a relatively low melting point (i.e., 60 °C), and solubility in several common solvents (e.g., chloroform, acetone, and dimethylformamide). Moreover, PCL is a low-cost polymer that has no isomers; hence, it has distinct biological degradation and melting points for different variants [208–210]. Electrospun nonwoven membranes of PCL and chitosan were shown to exhibit significant differences in cell proliferation depending on the fabrication technique. For instance, scaffolds fabricated by simultaneous deposition of PCL and CS fibers electrospun from separate solutions resulted in doubled proliferation rate compared to those fabricated by blending the solutions of both polymers followed by electrospinning [211]. PCL fibers were recently successfully used to culture H125 Lung adenosquamous carcinomas spheroids [212]. One major concern with synthetic polymers is the need for toxic chemicals to break bonds within the matrix, which make the release of spheroids after formation much more challenging. PCL was shown to be a potential candidate polymer in COVID-19 studies. For instance, Rezaei et al. developed 3D printed scaffold for engineering lung tissue using PCL bioink. The scaffold showed significant improvement in degradation, swelling, and mechanical characteristics. In addition, the scaffold protected the cells from apoptosis, and promoted cell adhesion, high proliferation, and cell biocompatibility in vitro [213]. In another study, Dye et al. developed adult airway epithelial cell model using PEG and PCL. In contrast to PEG that inhibited growth and maturation of cells at the immature lung progenitor stage, PLC allowed maturation of the organoids to tube-like structures, resembling the structure and diversity of cells in the adult airways [214]. These studies show the promising potential of using PLC scaffold to generate 3D lung models for SARS-CoV-2 studies (Table 2).

Limitations of 3D cell culture models

Despite being a promising and more physiologically relevant technique, 3D culture systems showed some limitations. For example, spheroids were reported to have variable size and diameter, unequal distribution of oxygen, nutrients and paracrine factors and self-disassembly due to factors' consumption [223–226]. In addition, 3D culture models are expensive and time and effort consuming when compared to 2D culture systems [227–229], and showed less sensitivity to treatments in drug discoveries and drug repositioning experiments [230, 231]. Despite being more biomimetic than 2D culture models, 3D models have been reported to be hard to reach to in vivo maturity [232], and some 3D models lack essential type of cells that are difficult to be involved in the culture system [232]. It is worth mentioning that each model has its own limitations based on the used cell types, ECM, and different culture conditions. For example, hydrogel models showed difficulties in culture medium change and cell harvesting [233, 234]. On the other hand, hanging droplet models are much more time and effort consuming with no ECM–cell interaction, and difficult transfer to the formed spheroids for the required analysis, in addition to heightened sensitivity to mechanical stress [235, 236]. Other limitations to 3D culture models include difficult fabrication for the ECM and the entire system, and difficult visualization due to the multicellular composition of the model [231, 236].

Conclusions and future prospective

3D lung models are promising biomimetic models for drug screening and various in vitro studies for the current SARS-CoV-2. Despite the rapid progress in developing 3D tissue models, many technical challenges still prevent their full application in pathogen infection studies. Importantly, further studies are required to determine the best type of cells to accomplish the most physiologically relevant microenvironment for lung modeling. In addition, inadequate vasculization and precipitous core necrosis of the current 3 D lung organoids call for better techniques to maintain adequate nutrition and enduring vascularization. This can be achieved by inclusion of vascular ECs or progenitors such as PCs. Scaffold material also need further optimization, as both natural and synthetic polymers have their individual shortcomings. Natural polymers lack the characteristic mechanical properties and the required reproducibility. On the other hand, the absence of ECM components in synthetic polymers and their inertness limit their use. Integrating bioactive peptides into synthetic polymers could facilitate their use in the generation of 3D lung models. In addition, combining both natural and synthetic scaffolds in a single composite polymer represents a valid, widely applicable solution to overcome the shortcomings of each polymer individually. Studies on PDMS and HA have also shown their promising applications in generating 3D lung model and may present achievable and reliable means for better studies of lung infections and therapy. The above-mentioned techniques of 3D in vitro lung models, such as spheroids, organoids, and organ-on-a-chip can be used to better understand the underlying mechanisms of COVID-19 infection, including how the virus interacts with human cells and how it causes disease. By providing a more accurate representation of the in vivo microenvironment, these models can also be used to test the efficacy of potential antiviral drugs and to identify new drug targets. Furthermore, 3D in vitro lung models can be used to study the long-term effects of the virus on the lung tissue, which can be applied for the development of treatments for post-acute sequelae of COVID-19. They can also be used to study the effects of exposure to environmental toxins, such as air pollution, which may exacerbate the disease. Overall, 3D in vitro lung models can provide a powerful tool for understanding the underlying mechanisms of COVID-19 infection and for identifying new therapeutics to combat the disease.

Abbreviations

COVID-19	Corona virus disease of 2019
2D	Two-dimensional
3D	Three-dimensional
SARS-CoV-2	Severe acute respiratory syndrome coronavirus 2
HD	Hanging drop method
PDT	Photodynamic therapy
EGF	Epidermal growth factor
NHBEs	Normal human bronchial epithelial cells
ROCKi	Rho-associated protein kinase inhibitors
ECs	Endothelial cells
RSV	Respiratory syncytial virus
ECM	Extracellular matrix
AEC2	Type II alveolar epithelial cells
FGF7	Fibroblast growth factor 7
GSK-3β	Glycogen synthase kinase 3
TGF-β	Transforming growth factor beta
BMP4	Bone morphogenetic protein 4
AT1	Alveolar type 1
AT2	Alveolar type 2
PNECs	Pulmonary neuroendocrine cells
BASCs	Bronchioalveolar stem cells
AEC1	Alveolar epithelial type I
NGFR	Nerve-growth factor receptor
hPSCs	Human pluripotent stem cells
ACE2	Angiotensin-converting enzyme 2
TMPRSS2	Transmembrane serine protease 2
hPSC-LOs	Lung organoid model from human pluripotent stem cells
hAT2	Human alveolar stem cells
IFNs	Interferons
hBO	Human bronchial organoids
GFR	Growth factor reduced
ALI	Air–liquid interface
hiPSCs	Human-induced pluripotent stem cells
hAWOs	Human airway organoids
hALOs	Alveolar organoids

hESCs	Human embryonic stem cells
VEGF	Vascular endothelia growth factor
Dll4	Delta-like ligand 4
MMP	Matrix metalloproteinase
ECs	Endothelial cells
HIF-1	Hypoxia-inducible factor-1
ERK-1/2	Extracellular regulating kinase 1/2
MEK-1/2	Mitogen-activated protein kinase 1/2
PCs	Pericytes
HUVEC	Human umbilical vein endothelial cells
HUASC	Human umbilical artery smooth muscle cells
PDGF-B	Platelet-derived growth factor beta
DECs	Dermal endothelial cell
HDFs	Human dermal fibroblasts
MPCs	Mesodermal progenitor cells
CAM	Chicken chorion allantois membrane
EPCs	Endothelial progenitor cells
NG2	Neuron-glial antigen 2
α-SMA	Alpha-smooth muscle actin
MSCs	Mesenchymal stromal cells
bFGF	Basic fibroblast growth factor
ETV2	Erythroblast transformation-specific transcription factor 2
BM-MSCs	Bone marrow mesenchymal stem cells
GAG	Glycosaminoglycan
SF	Silk fibroin
UC-MSCs	Human umbilical cord MSCs
ASCs	Adipose stem cells
PEG	Polyethylene glycol
RGD	Arginine–glycine–aspartate–serine peptide
IGF-1	Insulin-like growth factor-1
TGF-β	Transforming growth factor beta
NGF	Nerve-growth factor
LSCs	Lung spheroid cells
RSV	Respiratory syncytial virus
HA	Hyaluronic acid
RHAMM	Receptor for hyaluronan-mediated motility
ICAM-1	Intercellular adhesion molecule 1
OCT3/4	Octamer-binding transcription factor 3/4
SOX-2	Sex-determining region Y HMG-box 2
SSEA-3	Stage-specific embryonic antigen 3
HA–CS	Hyaluronan–chitosan
HSAECs	Human small airway epithelial cells
RGD	Arginylglycylaspartic acid
RGDS	Arginine–glycine–aspartate–serine peptide
MMP-2	Matrix metalloproteinase-2
MMP-9	Matrix metalloproteinase-9
PNIPAm	Poly(N-isopropylacrylamide)
HLF	Human lung fibroblast
PDMS	Polydimethylsiloxane
PCL	Poly-ϵ caprolactone

Acknowledgements
Not applicable.

Author contributions
TA conceived the idea and helped in data collection and writing the paper, BE, SE, HE, AME, and MFE contributed to writing the paper, NE was responsible for the overall conception and completion of the project and editing the manuscript. All authors read and approved the final manuscript.

Funding
Open access funding provided by The Science, Technology & Innovation Funding Authority (STDF) in cooperation with The Egyptian Knowledge Bank (EKB). This project was funded by a grant from the Academy of Scientific Research and Technology (ASRT), Project # ASRT 7304, Ministry of Scientific Research, Egypt.

Availability of data and materials
All data presented in this review are available and present in the text.

Declarations

Ethics approval and consent to participate
Not applicable.

Consent for publication
Not applicable.

Competing interests
The authors declare no competing interests.

Received: 15 October 2022 Accepted: 14 April 2023
Published online: 28 April 2023

References

1. Shi J, et al. Challenges of drug development during the COVID-19 pandemic: Key considerations for clinical trial designs. Br J Clin Pharmacol. 2021;87(5):2170–85. https://doi.org/10.1111/bcp.14629.
2. Hu B, Guo H, Zhou P, Shi Z-L. Characteristics of SARS-CoV-2 and COVID-19. Nat Rev Microbiol. 2021;19(3):141–54. https://doi.org/10.1038/s41579-020-00459-7.
3. Duval K, et al. Modeling physiological events in 2D vs. 3D cell culture. Physiology. 2017;32:266–77.
4. Booij TH, Price LS, Danen EHJ. 3D cell-based assays for drug screens: challenges in imaging, image analysis, and high-content analysis. SLAS Discov. 2019;24:615–27.
5. Steele VE, Lubet RA. The use of animal models for cancer chemoprevention drug development. Semin Oncol. 2010;37(4):327–38. https://doi.org/10.1053/j.seminoncol.2010.05.010.
6. Antoni D, Burckel H, Josset E, Noel G. Three-dimensional cell culture: a breakthrough in vivo. Int J Mol Sci. 2015;16(12):5517–27. https://doi.org/10.3390/ijms16035517.
7. Qian X, Song H, Ming G-L. Brain organoids: advances, applications and challenges. Development. 2019;146(8):dev166074. https://doi.org/10.1242/dev.166074.
8. Chen HI, Song H, Ming G-L. Applications of human brain organoids to clinical problems. Dev Dyn. 2019;248(1):53–64. https://doi.org/10.1002/dvdy.24662.
9. Russell WMS, Burch RL. The principles of humane experimental technique. The principles of humane experimental technique. London: Methuen & Co. Ltd. (1959)
10. Kelm JM, Timmins NE, Brown CJ, Fussenegger M, Nielsen LK. Method for generation of homogeneous multicellular tumor spheroids applicable to a wide variety of cell types. Biotechnol Bioeng. 2003;83:173–80.
11. Ryu NE, Lee SH, Park H. Spheroid culture system methods and applications for mesenchymal stem cells. Cells. 2019;8:1620.
12. Prytherch Z, Job C, Marshall H, Oreffo V, Foster M, BéruBé K. Tissue-specific stem cell differentiation in an in vitro airway model. Macromol Biosci. 2011;11:e66417.
13. Chua RL, et al. Cross-talk between the airway epithelium and activated immune cells defines severity in COVID-19 (2020).
14. He B, Chen G, Zeng Y. REVIEW Three-dimensional cell culture models for investigating human viruses. Virol Sin. 2016;31:363–79.
15. Benali R, Chevillard M, Zahm JM, Hinnrasky J, Klossek JM, Puchelle E. Tubule formation and functional differentiation by human epithelial respiratory cells cultured in a three-dimensional collagen matrix.
16. Vinci M, et al. Advances in establishment and analysis of three-dimensional tumor spheroid-based functional assays for target validation and drug evaluation. BMC Biol. 2012;10:29.
17. Kim SJ, et al. Hydrogels with an embossed surface: an all-in-one platform for mass production and culture of human adipose-derived stem cell spheroids. Biomaterials. 2019;188:198–212.
18. Raredon MSB, Ghaedi M, Calle EA, Niklason LE. A rotating bioreactor for scalable culture and differentiation of respiratory epithelium. Cell Med. 2015;7:109–21.
19. Timmins NE, Nielsen LK. Generation of multicellular tumor spheroids by the hanging-drop method. Methods Mol Med. 2007;140:141–51.

20. Patra B, Peng C-C, Liao W-H, Lee C-H, Tung Y-C. Drug testing and flow cytometry analysis on a large number of uniform sized tumor spheroids using a microfluidic device OPEN. Nature Publishing Group (2016)
21. Ivascu A, Kubbies M. Rapid generation of single-tumor spheroids for high-throughput cell function and toxicity analysis (2006)
22. Liu FF, et al. Hanging drop: an in vitro air toxic exposure model using human lung cells in 2D and 3D structures. J Hazard Mater. 2013;261:701–10.
23. Delgado O, et al. Multipotent capacity of immortalized human bronchial epithelial cells. PLoS ONE. 2011;6:e22023.
24. Jedrych E, et al. Evaluation of cytotoxic effect of 5-fluorouracil on human carcinoma cells in microfluidic system. Sens Actuators B Chem. 2011;160:1544–51.
25. Zuchowska A, Jastrzebska E, Chudy M, Dybko A, Brzozka Z. 3D lung spheroid cultures for evaluation of photodynamic therapy (PDT) procedures in microfluidic Lab-on-a-Chip system. Anal Chim Acta. 2017;990:110–20.
26. Kimura J, Deutsch GH. Key mechanisms of early lung development. Pediatr Dev Pathol. 2007;10:335–47.
27. Hagiwara M, Nakase I. Epidermal growth factor induced macropinocytosis directs branch formation of lung epithelial cells. Biochem Biophys Res Commun. 2018;507(1):297–303. https://doi.org/10.1016/j.bbrc.2018.11.028.
28. Horani A, Nath A, Wasserman MG, Huang T, Brody SL. Rho-associated protein kinase inhibition enhances airway epithelial basal-cell proliferation and lentivirus transduction. Am J Respir Cell Mol Biol. 2013;49:341–7.
29. Butler CR, et al. Rapid expansion of human epithelial stem cells suitable for airway tissue engineering. Am J Respir Crit Care Med. 2016;194(2):156–68. https://doi.org/10.1164/rccm.201507-1414oc.
30. Yamada KM, Cukierman E. Modeling tissue morphogenesis and cancer in 3D. Cell. 2007;130:601–10.
31. Kumari N, Bhargava A, Rath SN. T-type calcium channel antagonist, TTA-A2 exhibits anti-cancer properties in 3D spheroids of A549, a lung adenocarcinoma cell line. Life Sci. 2020;260:118291.
32. Saleh F, Harb A, Soudani N, Zaraket H. A three-dimensional A549 cell culture model to study respiratory syncytial virus infections. J Infect Public Health. 2020;13:1142–7.
33. Abdul L, et al. Deep-LUMEN assay-human lung epithelial spheroid classification from brightfield images using deep learning. Lab Chip. 2020;20:4623–31.
34. Carterson AJ, et al. A549 lung epithelial cells grown as three-dimensional aggregates: Alternative tissue culture model for Pseudomonas aeruginosa pathogenesis. Infect Immun. 2005;73:1129–40.
35. Van Riet S et al. In vitro modelling of alveolar repair at the air-liquid interface using alveolar epithelial cells derived from human induced pluripotent stem cells. Sci Rep. 10(1) (2020). https://doi.org/10.1038/s41598-020-62226-1.
36. Shiraishi K, Nakajima T, Shichino S, Deshimaru S, Matsushima K, Ueha S. In vitro expansion of endogenous human alveolar epithelial type II cells in fibroblast-free spheroid culture. Biochem Biophys Res Commun. 2019;515:579–85.
37. Dinh PUC, et al. Derivation of therapeutic lung spheroid cells from minimally invasive transbronchial pulmonary biopsies. Respir Res. 2017;18:1–11.
38. Rock JR, et al. Basal cells as stem cells of the mouse trachea and human airway epithelium. Proc Natl Acad Sci USA. 2009;106:12771–5.
39. Schoch KG, Lori A, Burns KA, Eldred T, Olsen JC, Randell SH. A subset of mouse tracheal epithelial basal cells generates large colonies in vitro. Am J Physiol Lung Cell Mol Physiol. 2004;286:631–42.
40. Barkauskas CE, et al. Type 2 alveolar cells are stem cells in adult lung. J Clin Investig. 2013;123:3025–36.
41. Cutz E. Neuroendocrine cells of the lung an overview of morphologic characteristics and development. Exp Lung Res. 1982;3:185–208.
42. Lee JH, et al. Lung stem cell differentiation in mice directed by endothelial cells via a BMP4-NFATc1-thrombospondin-1 axis. Cell. 2014;156:440–55.
43. Jones-Freeman B, Starkey MR. Bronchioalveolar stem cells in lung repair, regeneration and disease. J Pathol. 2020;252:219–26.
44. Gotoh S, et al. Generation of alveolar epithelial spheroids via isolated progenitor cells from human pluripotent stem cells. Stem Cell Rep. 2014;3:394–403.
45. Dye BR, et al. In vitro generation of human pluripotent stem cell derived lung organoids. Elife. 2015;2015:1–25.
46. McCauley KB, Hawkins F, Serra M, Thomas DC, Jacob A, Kotton DN. Efficient derivation of functional human airway epithelium from pluripotent stem cells via temporal regulation of Wnt signaling. Cell Stem Cell. 2017;20:844-857.e6.
47. Vaart J, Clevers H. Airway organoids as models of human disease. J Intern Med. 2020;289(5):604–13.
48. Lukiw WJ, Pogue A, Hill JM. SARS-CoV-2 infectivity and neurological targets in the brain. Cell Mol Neurobiol. 2020. https://doi.org/10.1007/s10571-020-00947-7.
49. Li S, et al. SARS-CoV-2: mechanism of infection and emerging technologies for future prospects. Rev Med Virol. 2021;31(2):2168. https://doi.org/10.1002/rmv.2168.
50. Reza-Zaldívar EE, et al. Infection mechanism of SARS-COV-2 and Its implication on the nervous system. Front Immunol. 2021. https://doi.org/10.3389/fimmu.2020.621735.
51. Lamers MM, et al. SARS-CoV-2 productively infects human gut enterocytes. Science. 2020;369:50–4.
52. Youk J, Kim T, Evans KV, Choi B-S, Ju YS, Lee J-H. Three-dimensional human alveolar stem cell culture models reveal infection response to SARS-CoV-2 (2020)
53. Zhao B, et al. Recapitulation of SARS-CoV-2 infection and cholangiocyte damage with human liver ductal organoids. Protein Cell. 2020;11:771–5.
54. Fan Z, et al. Clinical features of COVID-19-related liver functional abnormality. Clin Gastroenterol Hepatol. 2020;18:1561–6.
55. Li Z, et al. Caution on kidney dysfunctions of COVID-19 patients. medRxiv, ed: medRxiv (2020) p. 2020.02.08.20021212.
56. Zheng YY, Ma YT, Zhang JY, Xie X. COVID-19 and the cardiovascular system. Nat Rev Cardiol. 2020;17:259–60.
57. Gavriatopoulou M, et al. Organ-specific manifestations of COVID-19 infection. Clin Exp Med. 2020;20:493–506.
58. Han Y, et al. Identification of SARS-CoV-2 inhibitors using lung and colonic organoids. Nature. 2021;589:270–5.
59. Salahudeen AA, et al. Progenitor identification and SARS-CoV-2 infection in human distal lung organoids. Nature. 2020;588:670–5.
60. Katsura H, et al. Human lung stem cell-based alveolospheres provide insights into SARS-CoV-2-mediated interferon responses and pneumocyte dysfunction. Cell Stem Cell. 2020;27:890-904.e8.
61. Suzuki T, et al. Generation of human bronchial organoids for SARS-CoV-2 research. bioRxiv 4, 2020.05.25.115600 (2020)
62. Velasco V, Shariati SA, Esfandyarpour R. Microtechnology-based methods for organoid models. Microsyst Nanoeng. 2020;6:1–13.
63. Si L, et al. Human organs-on-chips as tools for repurposing approved drugs as potential influenza and COVID19 therapeutics in viral pandemics
64. Tindle C, et al. Adult stem cell-derived complete lung organoid models emulate lung disease in COVID-19. bioRxiv: the preprint server for biology, p. 2020.10.17.344002 (2020)
65. Chen Y, et al. Long-term engraftment promotes differentiation of alveolar epithelial cells from human embryonic stem cell derived lung organoids. Stem Cells Dev. 2018;27:1339–49.
66. Pei R, et al. Human embryonic stem cell-derived lung organoids: a model for SARS-CoV-2 infection and drug test. bioRxiv, p. 2020.08.10.244350 (2020)
67. Mulay A, et al. SARS-CoV-2 infection of primary human lung epithelium for COVID-19 modeling and drug discovery. bioRxiv, p. 2020.06.29.174623 (2020)
68. Samuel RM, et al. Androgen signaling regulates SARS-CoV-2 receptor levels and is associated with severe COVID-19 symptoms in men. Cell Stem Cell. 2020;27:876-889.e12.
69. Coultas L, Chawengsaksophak K, Rossant J. Endothelial cells and VEGF in vascular development. Nature. 2005;438(7070):937–45.
70. El-Derby AM, Ahmed TA, Abd El-Hameed AM, Elkhenany H, Saad SM, El-Badri N. Adult stem cells: mesenchymal stromal cells, endothelial progenitor cells, and pericytes. In: Regenerative medicine and stem cell biology. Springer, pp. 109–149 (2020)

71. Patel-Hett S, D'Amore PA. Signal transduction in vasculogenesis and developmental angiogenesis. Int J Dev Biol. 2011;55:353.
72. Bautch VL, Caron KM. Blood and lymphatic vessel formation. Cold Spring Harb Perspect Biol. 2015;7(3):a008268.
73. Park C, Kim TM, Malik AB. Transcriptional regulation of endothelial cell and vascular development. Circ Res. 2013;112(10):1380–400.
74. Keller G. Embryonic stem cell differentiation: emergence of a new era in biology and medicine. Genes Dev. 2005;19(10):1129–55.
75. Jakobsson L, et al. Endothelial cells dynamically compete for the tip cell position during angiogenic sprouting. Nat Cell Biol. 2010;12(10):943–53.
76. Hellström M, et al. Dll4 signalling through Notch1 regulates formation of tip cells during angiogenesis. Nature. 2007;445(7129):776–80.
77. Kamei M, Saunders WB, Bayless KJ, Dye L, Davis GE, Weinstein BM. Endothelial tubes assemble from intracellular vacuoles in vivo. Nature. 2006;442(7101):453–6.
78. Blum Y, Belting H-G, Ellertsdottir E, Herwig L, Lüders F, Affolter M. Complex cell rearrangements during intersegmental vessel sprouting and vessel fusion in the zebrafish embryo. Dev Biol. 2008;316(2):312–22.
79. Swift MR, Weinstein BM. Arterial–venous specification during development. Circ Res. 2009;104(5):576–88.
80. Van Dijk CG, et al. The complex mural cell: pericyte function in health and disease. Int J Cardiol. 2015;190:75–89.
81. Carmeliet P, Jain RK. Molecular mechanisms and clinical applications of angiogenesis. Nature. 2011;473(7347):298–307.
82. Daneman R, Zhou L, Kebede AA, Barres BA. Pericytes are required for blood–brain barrier integrity during embryogenesis. Nature. 2010;468(7323):562–6.
83. Ahmed TA, El-Badri N. Pericytes: the role of multipotent stem cells in vascular maintenance and regenerative medicine. Cell Biol Transl Med. 2017;1:69–86.
84. Rouwkema J, Rivron NC, van Blitterswijk CA. Vascularization in tissue engineering. Trends Biotechnol. 2008;26(8):434–41.
85. Burr S, et al. Oxygen gradients can determine epigenetic asymmetry and cellular differentiation via differential regulation of Tet activity in embryonic stem cells. Nucleic Acids Res. 2018;46(3):1210–26.
86. Tsigkou O, et al. Engineered vascularized bone grafts. Proc Natl Acad Sci. 2010;107(8):3311–6.
87. Chen L, et al. Pre-vascularization enhances therapeutic effects of human mesenchymal stem cell sheets in full thickness skin wound repair. Theranostics. 2017;7(1):117.
88. Wörsdörfer P, et al. Generation of complex human organoid models including vascular networks by incorporation of mesodermal progenitor cells. Sci Rep. 2019;9(1):1–13.
89. Jakab K, et al. Tissue engineering by self-assembly of cells printed into topologically defined structures. Tissue Eng Part A. 2008;14(3):413–21.
90. Inamori M, Mizumoto H, Kajiwara T. An approach for formation of vascularized liver tissue by endothelial cell–covered hepatocyte spheroid integration. Tissue Eng Part A. 2009;15(8):2029–37.
91. Grebenyuk S, Ranga A. Engineering organoid vascularization. Front Bioeng Biotechnol. 2019;7:39.
92. Czajka CA, Drake CJ. Self-assembly of prevascular tissues from endothelial and fibroblast cells under scaffold-free, nonadherent conditions. Tissue Eng Part A. 2015;21(1–2):277–87.
93. Levenberg S, et al. Engineering vascularized skeletal muscle tissue. Nat Biotechnol. 2005;23(7):879–84.
94. Chen YC, et al. Functional human vascular network generated in photocrosslinkable gelatin methacrylate hydrogels. Adv Funct Mater. 2012;22(10):2027–39.
95. Korff T, Augustin HG. Integration of endothelial cells in multicellular spheroids prevents apoptosis and induces differentiation. J Cell Biol. 1998;143(5):1341–52.
96. Pham MT, et al. Generation of human vascularized brain organoids. NeuroReport. 2018;29(7):588.
97. Noguchi R, et al. Development of a three-dimensional pre-vascularized scaffold-free contractile cardiac patch for treating heart disease. J Heart Lung Transplant. 2016;35(1):137–45.
98. Okudaira T, Amimoto N, Mizumoto H, Kajiwara T. Formation of three-dimensional hepatic tissue by the bottom-up method using spheroids. J Biosci Bioeng. 2016;122(2):213–8.
99. Wang Z, He Y, Yu X, Fu W, Wang W, Huang H. Rapid vascularization of tissue-engineered vascular grafts in vivo by endothelial cells in co-culture with smooth muscle cells. J Mater Sci Mater Med. 2012;23(4):1109–17.
100. Korff T, Kimmina S, Martiny-Baron G, Augustin HG. Blood vessel maturation in a 3-dimensional spheroidal coculture model: direct contact with smooth muscle cells regulates endothelial cell quiescence and abrogates VEGF responsiveness. FASEB J. 2001;15(2):447–57.
101. Garzoni LR, et al. Dissecting coronary angiogenesis: 3D co-culture of cardiomyocytes with endothelial or mesenchymal cells. Exp Cell Res. 2009;315(19):3406–18.
102. Dohle E, et al. Macrophage-mediated angiogenic activation of outgrowth endothelial cells in co-culture with primary osteoblasts. Eur Cell Mater. 2014;27(149–164):164–5.
103. Walser R, Metzger W, Görg A, Pohlemann T, Menger M, Laschke M. Generation of co-culture spheroids as vascularisation units for bone tissue engineering. Eur Cell Mater. 2013;26:222–33.
104. Asahara T, et al. Isolation of putative progenitor endothelial cells for angiogenesis. Science. 1997;275(5302):964–6.
105. Loibl M, et al. Direct cell-cell contact between mesenchymal stem cells and endothelial progenitor cells induces a pericyte-like phenotype in vitro. BioMed Res Int 2014 (2014)
106. Duttenhoefer F, et al. 3D scaffolds co-seeded with human endothelial progenitor and mesenchymal stem cells: evidence of prevascularisation within 7 days. Eur Cells Mater eCM. 2013;26:64–5.
107. Wang N, et al. Vascular endothelial growth factor stimulates endothelial differentiation from mesenchymal stem cells via Rho/myocardin-related transcription factor-A signaling pathway. Int J Biochem Cell Biol. 2013;45(7):1447–56.
108. Au P, Tam J, Fukumura D, Jain RK. Bone marrow–derived mesenchymal stem cells facilitate engineering of long-lasting functional vasculature. Blood. 2008;111(9):4551–8.
109. Laranjeira M, Fernandes M, Monteiro F. Reciprocal induction of human dermal microvascular endothelial cells and human mesenchymal stem cells: time-dependent profile in a co-culture system. Cell Prolif. 2012;45(4):320–34.
110. Kolbe M, Xiang Z, Dohle E, Tonak M, Kirkpatrick CJ, Fuchs S. Paracrine effects influenced by cell culture medium and consequences on microvessel-like structures in cocultures of mesenchymal stem cells and outgrowth endothelial cells. Tissue Eng Part A. 2011;17(17–18):2199–212.
111. Stenderup K, Justesen J, Clausen C, Kassem M. Aging is associated with decreased maximal life span and accelerated senescence of bone marrow stromal cells. Bone. 2003;33(6):919–26.
112. Wu X, et al. Mesenchymal stem cells participating in ex vivo endothelium repair and its effect on vascular smooth muscle cells growth. Int J Cardiol. 2005;105(3):274–82.
113. Deegan AJ, Hendrikson WJ, El Haj AJ, Rouwkema J, Yang Y. Regulation of endothelial cell arrangements within hMSC–HUVEC co-cultured aggregates. Biomed J. 2019;42(3):166–77.
114. Morita R, et al. ETS transcription factor ETV2 directly converts human fibroblasts into functional endothelial cells. Proc Natl Acad Sci. 2015;112(1):160–5.
115. Wang K, et al. Robust differentiation of human pluripotent stem cells into endothelial cells via temporal modulation of ETV2 with modified mRNA. Sci Adv. 2020;6(30):eaba7606.
116. Cakir B, et al. Engineering of human brain organoids with a functional vascular-like system. Nat Methods. 2019;16(11):1169–75.
117. Elkhenany H, Abd Elkodous M, Newby SD, El-Derby AM, Dhar M, El-Badri N. Tissue engineering modalities and nanotechnology. In: Regenerative medicine and stem cell biology. Springer, pp. 289–322 (2020)
118. El-Badri N, Elkhenany H. Toward the nanoengineering of mature, well-patterned and vascularized organoids. Nanomedicine. 2021;16(15):1255–8. https://doi.org/10.2217/nnm-2021-0074.
119. Laurent G. Lung collagen: more than scaffolding. Thorax. 1986;41(6):418.
120. Nagaishi C, Nagaishi C, Nagasawa N. Functional anatomy and histology of the lung. Philadelphia: University Park Press; 1972.
121. Turino G, Lourenco R. The connective tissue basis of pulmonary mechanics. In: Pulmonary emphysema and proteolysis. Academic Press, New York, p 509 (1972)
122. Hamilton NJI, et al. Using a three-dimensional collagen matrix to deliver respiratory progenitor cells to decellularized trachea in vivo. Tissue Eng

Part C Methods. 2019;25(2):93–102. https://doi.org/10.1089/ten.TEC.2018.0241.
123. Rashedi I, Talele N, Wang X-H, Hinz B, Radisic M, Keating A. Collagen scaffold enhances the regenerative properties of mesenchymal stromal cells. PLoS ONE. 2017;12(10):e0187348. https://doi.org/10.1371/journal.pone.0187348.
124. Elkhenany HA, et al. Bone marrow mesenchymal stem cell-derived tissues are mechanically superior to meniscus cells. Tissue Eng Part A (2020)
125. Stejskalová A, et al. Collagen I triggers directional migration, invasion and matrix remodeling of stroma cells in a 3D spheroid model of endometriosis. Sci Rep. 2021;11(1):4115. https://doi.org/10.1038/s41598-021-83645-8.
126. Chen P, Marsilio E, Goldstein RH, Yannas IV, Spector M. Formation of lung alveolar-like structures in collagen-glycosaminoglycan scaffolds in vitro. Tissue Eng. 2005;11(9–10):1436–48. https://doi.org/10.1089/ten.2005.11.1436.
127. Lee SW, et al. In vitro lung cancer multicellular tumor spheroid formation using a microfluidic device. Biotechnol Bioeng. 2019;116(11):3041–52. https://doi.org/10.1002/bit.27114.
128. Rockwood DN, Preda RC, Yücel T, Wang X, Lovett ML, Kaplan DL. Materials fabrication from Bombyx mori silk fibroin. Nat Protoc. 2011;6(10):1612–31. https://doi.org/10.1038/nprot.2011.379.
129. Vepari C, Kaplan DL. Silk as a biomaterial. Prog Polym Sci. 2007;32(8–9):991–1007. https://doi.org/10.1016/j.progpolymsci.2007.05.013.
130. Zhang L, Liu X, Li G, Wang P, Yang Y. Tailoring degradation rates of silk fibroin scaffolds for tissue engineering. J Biomed Mater Res Part A. 2019;107(1):104–13. https://doi.org/10.1002/jbm.a.36537.
131. Chen Z, et al. Porous three-dimensional silk fibroin scaffolds for tracheal epithelial regeneration in vitro and in vivo. ACS Biomater Sci Eng. 2018;4(8):2977–85. https://doi.org/10.1021/acsbiomaterials.8b00419.
132. Millán-Rivero JE, et al. Silk fibroin scaffolds seeded with Wharton's jelly mesenchymal stem cells enhance re-epithelialization and reduce formation of scar tissue after cutaneous wound healing. Stem Cell Res Therapy. 2019;10(1):126. https://doi.org/10.1186/s13287-019-1229-6.
133. Watchararot T, Prasongchean W, Thongnuek P. Angiogenic property of silk fibroin scaffolds with adipose-derived stem cells on chick chorioallantoic membrane. R Soc Open Sci. 2021;8(3):201618.
134. Mosesson MW, Siebenlist KR, Meh DA. The structure and biological features of fibrinogen and fibrin. Ann N Y Acad Sci. 2001;936(1):11–30.
135. Swartz DD, Russell JA, Andreadis ST. Engineering of fibrin-based functional and implantable small-diameter blood vessels. Am J Physiol Heart Circ Physiol. 2005;288(3):H1451–60.
136. Sriram G, Bigliardi PL, Bigliardi-Qi M. Full-thickness human skin equivalent models of atopic dermatitis. In: Turksen K, editor. Skin stem cells: methods and protocols. New York: Springer; 2019. p. 367–83.
137. Sriram G, et al. Full-thickness human skin-on-chip with enhanced epidermal morphogenesis and barrier function. Mater Today. 2018;21(4):326–40.
138. Raghavan S, et al. Carcinoma-associated mesenchymal stem cells promote chemoresistance in ovarian cancer stem cells via PDGF signaling. Cancers. 2020;12(8):2063.
139. Mishra R, et al. Effect of prevascularization on in vivo vascularization of poly(propylene fumarate)/fibrin scaffolds. Biomaterials. 2016;77:255–66. https://doi.org/10.1016/j.biomaterials.2015.10.026.
140. Broguiere N, et al. Growth of epithelial organoids in a defined hydrogel. Adv Mater. 2018;30(43):1801621. https://doi.org/10.1002/adma.201801621.
141. Del Bufalo F, et al. 3D modeling of human cancer: A PEG-fibrin hydrogel system to study the role of tumor microenvironment and recapitulate the in vivo effect of oncolytic adenovirus. Biomaterials. 2016;84:76–85. https://doi.org/10.1016/j.biomaterials.2016.01.030.
142. Yanagisawa K, et al. A four-dimensional organoid system to visualize cancer cell vascular invasion. Biology (Basel). 2020;9(11):361. https://doi.org/10.3390/biology9110361.
143. Campos F, et al. Evaluation of fibrin-agarose tissue-like hydrogels biocompatibility for tissue engineering applications. Front Bioeng Biotechnol. 2020;8(596):1. https://doi.org/10.3389/fbioe.2020.00596.
144. Hughes CS, Postovit LM, Lajoie GA. Matrigel: a complex protein mixture required for optimal growth of cell culture. Proteomics. 2010;10(9):1886–90.
145. Orkin RW, Gehron P, McGoodwin EB, Martin GR, Valentine T, Swarm R. A murine tumor producing a matrix of basement membrane. J Exp Med. 1977;145(1):204–20. https://doi.org/10.1084/jem.145.1.204.
146. Vukicevic S, Kleinman HK, Luyten FP, Roberts AB, Roche NS, Reddi AH. Identification of multiple active growth factors in basement membrane Matrigel suggests caution in interpretation of cellular activity related to extracellular matrix components. Exp Cell Res. 1992;202(1):1–8. https://doi.org/10.1016/0014-4827(92)90397-q.
147. Kibbey MC. Maintenance of the EHS sarcoma and Matrigel preparation. J Tissue Cult Methods. 1994;16(3):227–30. https://doi.org/10.1007/BF01540656.
148. Diederichs S, Klampfleuthner FAM, Moradi B, Richter W. Chondral Differentiation of induced pluripotent stem cells without progression into the endochondral pathway. Front Cell Dev Biol. 2019;7:270. https://doi.org/10.3389/fcell.2019.00270.
149. Chen C, Rengarajan V, Kjar A, Huang Y. A matrigel-free method to generate matured human cerebral organoids using 3D-Printed microwell arrays. Bioact Mater. 2021;6(4):1130–9. https://doi.org/10.1016/j.bioactmat.2020.10.003.
150. Sorrentino G, et al. Mechano-modulatory synthetic niches for liver organoid derivation. Nat Commun. 2020;11(1):1–10.
151. Kulkeaw K, Tubsuwan A, Tongkrajang N, Whangviboonkij N. Generation of human liver organoids from pluripotent stem cell-derived hepatic endoderms. PeerJ. 2020;8:e9968.
152. Takasato M, et al. Kidney organoids from human iPS cells contain multiple lineages and model human nephrogenesis. Nature. 2015;526(7574):564–8.
153. Sato T, et al. Single Lgr5 stem cells build crypt-villus structures in vitro without a mesenchymal niche. Nature. 2009;459(7244):262–5. https://doi.org/10.1038/nature07935.
154. Fang Y, Eglen RM. Three-dimensional cell cultures in drug discovery and development. SLAS Discov Adv Life Sci R & D. 2017;22(5):456–72. https://doi.org/10.1177/1087057117696795.
155. Fang Y, Eglen RM. Three-dimensional cell cultures in drug discovery and development. Slas Discov Adv Life Sci R&D. 2017;22(5):456–72.
156. Anguiano M, et al. Characterization of three-dimensional cancer cell migration in mixed collagen-Matrigel scaffolds using microfluidics and image analysis. PLoS ONE. 2017;12(2):e0171417. https://doi.org/10.1371/journal.pone.0171417.
157. Miller AJ, et al. Generation of lung organoids from human pluripotent stem cells in vitro. Nat Protoc. 2019;14(2):518–40. https://doi.org/10.1038/s41596-018-0104-8.
158. Henry E, et al. Adult lung spheroid cells contain progenitor cells and mediate regeneration in rodents with bleomycin-induced pulmonary fibrosis. Stem Cells Transl Med. 2015;4(11):1265–74. https://doi.org/10.5966/sctm.2015-0062.
159. Banda M, McKim KL, Myers MB, Inoue M, Parsons BL. Outgrowth of erlotinib-resistant subpopulations recapitulated in patient-derived lung tumor spheroids and organoids. PLoS ONE. 2020;15(9):e0238862. https://doi.org/10.1371/journal.pone.0238862.
160. Padhye A, et al. A novel ex vivo tumor system identifies Src-mediated invasion and metastasis in mesenchymal tumor cells in non-small cell lung cancer. Sci Rep. 2019;9(1):4819. https://doi.org/10.1038/s41598-019-41301-2.
161. Kim M, et al. Patient-derived lung cancer organoids as in vitro cancer models for therapeutic screening. Nat Commun. 2019;10(1):3991. https://doi.org/10.1038/s41467-019-11867-6.
162. Souza-Fernandes AB, Pelosi P, Rocco PR. Bench-to-bedside review: the role of glycosaminoglycans in respiratory disease. Crit Care. 2006;10(6):237. https://doi.org/10.1186/cc5069.
163. Jamal RA, Roughley PJ, Ludwig MS. Effect of glycosaminoglycan degradation on lung tissue viscoelasticity. Am J Physiol-Lung Cell Mol Physiol. 2001;280(2):L306–15. https://doi.org/10.1152/ajplung.2001.280.2.L306.
164. Uhl FE, et al. Functional role of glycosaminoglycans in decellularized lung extracellular matrix. Acta Biomater. 2020;102:231–46. https://doi.org/10.1016/j.actbio.2019.11.029.
165. Hallak LK, Collins PL, Knudson W, Peeples ME. Iduronic acid-containing glycosaminoglycans on target cells are required for efficient respiratory syncytial virus infection. Virology. 2000;271(2):264–75. https://doi.org/10.1006/viro.2000.0293.

166. Kim E, et al. Paradoxical effects of chondroitin sulfate-E on Japanese encephalitis viral infection. Biochem Biophys Res Commun. 2011;409(4):717–22. https://doi.org/10.1016/j.bbrc.2011.05.072.
167. Kim SY, et al. Characterization of heparin and severe acute respiratory syndrome-related coronavirus 2 (SARS-CoV-2) spike glycoprotein binding interactions. Antiviral Res. 2020;181:104873. https://doi.org/10.1016/j.antiviral.2020.104873.
168. Fraser JR, Laurent TC, Laurent UB. Hyaluronan: its nature, distribution, functions and turnover. J Intern Med. 1997;242(1):27–33. https://doi.org/10.1046/j.1365-2796.1997.00170.x.
169. Entwistle J, Hall CL, Turley EA. HA receptors: regulators of signalling to the cytoskeleton. J Cell Biochem. 1996;61(4):569–77. https://doi.org/10.1002/(sici)1097-4644(19960616)61:4%3c569::aid-jcb10%3e3.0.co;2-b.
170. Park D, et al. Hyaluronic acid promotes angiogenesis by inducing RHAMM-TGFβ receptor interaction via CD44-PKCδ. Mol Cells. 2012;33(6):563–74. https://doi.org/10.1007/s10059-012-2294-1.
171. Liu A, et al. Therapeutic effects of hyaluronic acid in bacterial pneumonia in ex vivo perfused human lungs. Am J Respir Crit Care Med. 2019;200(10):1234–45.
172. Benedetti L, et al. Biocompatibility and biodegradation of different hyaluronan derivatives (Hyaff) implanted in rats. Biomaterials. 1993;14(15):1154–60. https://doi.org/10.1016/0142-9612(93)90160-4.
173. Brigham MD, Bick A, Lo E, Bendali A, Burdick JA, Khademhosseini A. Mechanically robust and bioadhesive collagen and photocrosslinkable hyaluronic acid semi-interpenetrating networks. Tissue Eng Part A. 2009;15(7):1645–53. https://doi.org/10.1089/ten.tea.2008.0441.
174. Feng J, et al. An injectable non-cross-linked hyaluronic-acid gel containing therapeutic spheroids of human adipose-derived stem cells. Sci Rep. 2017;7(1):1548–1548. https://doi.org/10.1038/s41598-017-01528-3.
175. Duranti F, Salti G, Bovani B, Calandra M, Rosati ML. Injectable hyaluronic acid gel for soft tissue augmentation. A clinical and histological study. Dermatol Surg. 1998;24(12):1317–25. https://doi.org/10.1111/j.1524-4725.1998.tb00007.x.
176. Kim IG, Cho H, Shin J, Cho JH, Cho SW, Chung EJ. Regeneration of irradiation-damaged esophagus by local delivery of mesenchymal stem-cell spheroids encapsulated in a hyaluronic-acid-based hydrogel. Biomater Sci. 2021;9(6):2197–208. https://doi.org/10.1039/d0bm01655a.
177. Han HW, Hsu SH. Chitosan-hyaluronan based 3D co-culture platform for studying the crosstalk of lung cancer cells and mesenchymal stem cells. Acta Biomater. 2016;42:157–67. https://doi.org/10.1016/j.actbio.2016.06.014.
178. Lodhi G, et al. Chitooligosaccharide and its derivatives: preparation and biological applications. Biomed Res Int. 2014;2014:654913–654913. https://doi.org/10.1155/2014/654913.
179. Nwe N, Furuike T, Tamura H. The mechanical and biological properties of chitosan scaffolds for tissue regeneration templates are significantly enhanced by chitosan from Gongronella butleri. Materials. 2009;2(2):374–98.
180. Madihally SV, Matthew HW. Porous chitosan scaffolds for tissue engineering. Biomaterials. 1999;20(12):1133–42. https://doi.org/10.1016/s0142-9612(99)00011-3.
181. Ma L, et al. Collagen/chitosan porous scaffolds with improved biostability for skin tissue engineering. Biomaterials. 2003;24(26):4833–41. https://doi.org/10.1016/s0142-9612(03)00374-0.
182. Kiuchi H, Kai W, Inoue Y. Preparation and characterization of poly (ethylene glycol) crosslinked chitosan films. J Appl Polym Sci. 2008;107(6):3823–30.
183. Bhowmick R, Derakhshan T, Liang Y, Ritchey J, Liu L, Gappa-Fahlenkamp H. A three-dimensional human tissue-engineered lung model to study influenza A infection. Tissue Eng Part A. 2018;24(19–20):1468–80. https://doi.org/10.1089/ten.TEA.2017.0449.
184. Park Y, Huh KM, Kang S-W. Applications of biomaterials in 3D cell culture and contributions of 3D cell culture to drug development and basic biomedical research. Int J Mol Sci. 2021;22(5):2491. https://doi.org/10.3390/ijms22052491.
185. Kamatar A, Gunay G, Acar H. Natural and synthetic biomaterials for engineering multicellular tumor spheroids. Polymers. 2020;12(11):2506.
186. Augst AD, Kong HJ, Mooney DJ. Alginate Hydrogels as Biomaterials. Macromol Biosci. 2006;6(8):623–33. https://doi.org/10.1002/mabi.200600069.
187. Hagel V, Haraszti T, Boehm H. Diffusion and interaction in PEG-DA hydrogels. Biointerphases. 2013;8:1–9.
188. Liang ZGJ, Timmerman A, Grijpma D, Poot A. Enhanced mechanical and cell adhesive properties of photo-crosslinked PEG hydrogels by incorporation of gelatin in the networks (2017), pp. 0–30.
189. Offeddu GS, Axpe E, Harley BAC, Oyen ML. Relationship between permeability and diffusivity in polyethylene glycol hydrogels. AIP Adv. 2018;8:105006.
190. Chapla R, Abed MA, West J. Modulating functionalized poly(Ethylene glycol) diacrylate hydrogel mechanical properties through competitive crosslinking mechanics for soft tissue applications. Polymers. 2020;12:1–16.
191. Gill BJ, et al. A synthetic matrix with independently tunable biochemistry and mechanical properties to study epithelial morphogenesis and EMT in a lung adenocarcinoma model. Can Res. 2012;72(22):6013–23.
192. Roudsari LC, Jeffs SE, Witt AS, Gill BJ, West JL. A 3D poly(ethylene glycol)-based tumor angiogenesis model to study the influence of vascular cells on lung tumor cell behavior. Sci Rep. 2016;6(1):32726. https://doi.org/10.1038/srep32726.
193. Nash ME, et al. Straightforward, one-step fabrication of ultrathin thermoresponsive films from commercially available pNIPAm for cell culture and recovery. ACS Appl Mater Interfaces. 2011;3:1980–90.
194. Nagase K, Yamato M, Kanazawa H, Okano T. Poly(N-isopropylacrylamide)-based thermoresponsive surfaces provide new types of biomedical applications. Biomaterials. 2018;153:27–48.
195. Dhamecha D, Le D, Chakravarty T, Perera K, Dutta A, Menon JU. Fabrication of PNIPAm-based thermoresponsive hydrogel microwell arrays for tumor spheroid formation. Mater Sci Eng C. 2021;125:112100.
196. Gu J, Zhao Y, Guan Y, Zhang Y. Effect of particle size in a colloidal hydrogel scaffold for 3D cell culture. Colloids Surf B. 2015;136:1139–47.
197. Xiong XC, Zhao D, Dai K, Xiao XC. Coaxial ring-layered poly(N-isopropylacrylamide) gel columns of improved thermoresponses. Mater Chem Phys. 2020;253:123421.
198. Capella V, et al. Cytotoxicity and bioadhesive properties of poly-N-isopropylacrylamide hydrogel. Heliyon. 2019;5:1–19.
199. Kim G, Jung Y, Cho K, Lee HJ, Koh WG. Thermoresponsive poly(N-isopropylacrylamide) hydrogel substrates micropatterned with poly(ethylene glycol) hydrogel for adipose mesenchymal stem cell spheroid formation and retrieval. Mater Sci Eng, C. 2020;115:111128.
200. Vignesh RA, Kumari S, Poddar P, Dhara D, Maiti S. Poly(N-isopropylacrylamide)-based polymers as additive for rapid generation of spheroid via hanging drop method. Macromol Biosci. 2020;20:1–10.
201. Anada T, Fukuda J, Sai Y, Suzuki O. An oxygen-permeable spheroid culture system for the prevention of central hypoxia and necrosis of spheroids. Biomaterials. 2012;33:8430–41.
202. Khot MI, et al. Characterising a PDMS based 3D cell culturing microfluidic platform for screening chemotherapeutic drug cytotoxic activity. Sci Rep. 2020;10:1–13.
203. Lim W, Park S. A microfluidic spheroid culture device with a concentration gradient generator for high-throughput screening of drug efficacy. Molecules. 2018;23:3355.
204. An HJ, Kim HS, Kwon JA, Song J, Choi I. Adjustable and versatile 3D tumor spheroid culture platform with interfacial elastomeric wells. ACS Appl Mater Interfaces. 2020;12:6924–32.
205. Lee D, Pathak S, Jeong JH. Design and manufacture of 3D cell culture plate for mass production of cell-spheroids. Sci Rep. 2019;9:1–8.
206. Roy N, Kashyap J, Verma D, Tyagi RK, Prabhakar A. Prototype of a smart microfluidic platform for the evaluation of SARS-Cov-2 pathogenesis, along with estimation of the effectiveness of potential drug candidates and antigen-antibody interactions in convalescent plasma therapy. Trans Indian Natl Acad Eng. 2020;5(2):241–50. https://doi.org/10.1007/s41403-020-00148-0.
207. Swank Z, et al. A high-throughput microfluidic nanoimmunoassay for detecting anti-SARS-CoV-2 antibodies in serum or ultralow-volume blood samples. Proc Natl Acad Sci USA. 2021;118(18):e2025289118. https://doi.org/10.1073/pnas.2025289118.
208. Cipitria A, Skelton A, Dargaville TR, Dalton PD, Hutmacher DW. Design, fabrication and characterization of PCL electrospun scaffolds - A review. J Mater Chem. 2011;21:9419–53.
209. Fuller KP, Gaspar D, Delgado LM, Pandit A, Zeugolis DI. Influence of porosity and pore shape on structural, mechanical and biological

properties of poly ϵ-caprolactone electro-spun fibrous scaffolds. Nanomedicine. 2016;11:1031–40.
210. Rabionet M, Yeste M, Puig T, Ciurana J. Electrospinning PCL scaffolds manufacture for three-dimensional breast cancer cell culture. Polymers. 2017;9:1–15.
211. Valente T, Ferreira JL, Henriques C, Borges JP, Silva JC. Polymer blending or fiber blending: a comparative study using chitosan and poly(ε-caprolactone) electrospun fibers. J Appl Polym Sci. 2019;136:1–11.
212. González-Martínez E, et al. Growing spheroids of lung adenosquamous carcinoma on electrospun poly(ε-caprolactone). Bioinspired Biomimetic Nanobiomater. 2020;9:252–6.
213. Rezaei FS, Khorshidian A, Beram FM, Derakhshani A, Esmaeili J, Barati A. 3D printed chitosan/polycaprolactone scaffold for lung tissue engineering: hope to be useful for COVID-19 studies. RSC Adv. 2021;11(32):19508–20. https://doi.org/10.1039/d1ra03410c.
214. Dye BR, et al. Human lung organoids develop into adult airway-like structures directed by physico-chemical biomaterial properties. Biomaterials. 2020;234:119757.
215. Dong C, Lv Y. Application of collagen scaffold in tissue engineering: recent advances and new perspectives. Polymers. 2016;8(2):42. https://doi.org/10.3390/polym8020042.
216. Litvinov RI, Weisel JW. Fibrin mechanical properties and their structural origins. Matrix Biol J Int Soc Matrix Biol. 2017;60–61:110–23. https://doi.org/10.1016/j.matbio.2016.08.003.
217. Greenlee AR, Kronenwetter-Koepel TA, Kaiser SJ, Ellis TM, Liu K. Combined effects of Matrigel and growth factors on maintaining undifferentiated murine embryonic stem cells for embryotoxicity testing. Toxicol In Vitro. 2004;18(4):543–53. https://doi.org/10.1016/j.tiv.2004.01.013.
218. Kane KI, et al. Determination of the rheological properties of Matrigel for optimum seeding conditions in microfluidic cell cultures. AIP Adv. 2018;8(12):125332.
219. Aisenbrey EA, Murphy WL. Synthetic alternatives to Matrigel. Nat Rev Mater. 2020;5(7):539–51. https://doi.org/10.1038/s41578-020-0199-8.
220. Zhu Z, Wang Y-M, Yang J, Luo X-S. Hyaluronic acid: a versatile biomaterial in tissue engineering. Plastic Aesthetic Res. 2017;4:219–27.
221. Dhiman HK, Ray AR, Panda AK. Characterization and evaluation of chitosan matrix for in vitro growth of MCF-7 breast cancer cell lines. Biomaterials. 2004;25(21):5147–54. https://doi.org/10.1016/j.biomaterials.2003.12.025.
222. Rodríguez-Vázquez M, Vega-Ruiz B, Ramos-Zúñiga R, Saldaña-Koppel DA, Quiñones-Olvera LF. Chitosan and its potential use as a scaffold for tissue engineering in regenerative medicine. Biomed Res Int. 2015;2015:821279–821279. https://doi.org/10.1155/2015/821279.
223. Achilli T-M, Meyer J, Morgan JR. Advances in the formation, use and understanding of multi-cellular spheroids. Expert Opin Biol Ther. 2012;12(10):1347–60.
224. Mueller-Klieser W. Three-dimensional cell cultures: from molecular mechanisms to clinical applications. Am J Physiol Cell Physiol. 1997;273(4):C1109–23.
225. Dhiman HK, Ray AR, Panda AK. Three-dimensional chitosan scaffold-based MCF-7 cell culture for the determination of the cytotoxicity of tamoxifen. Biomaterials. 2005;26(9):979–86.
226. Perche F, Patel NR, Torchilin VP. Accumulation and toxicity of antibody-targeted doxorubicin-loaded PEG–PE micelles in ovarian cancer cell spheroid model. J Control Release. 2012;164(1):95–102.
227. Breslin S, O'Driscoll L. Three-dimensional cell culture: the missing link in drug discovery. Drug Discovery Today. 2013;18(5–6):240–9.
228. Ricci C, Moroni L, Danti S. Cancer tissue engineering-new perspectives in understanding the biology of solid tumours-a critical review. OA Tissue Eng. 2013;1(4):1–4.
229. Habanjar O, Diab-Assaf M, Caldefie-Chezet F, Delort L. 3D cell culture systems: tumor application, advantages, and disadvantages. Int J Mol Sci. 2021;22(22):12200.
230. Lv D, Hu Z, Lu L, Lu H, Xu X. Three-dimensional cell culture: A powerful tool in tumor research and drug discovery. Oncol Lett. 2017;14(6):6999–7010.
231. Langhans SA. Three-dimensional in vitro cell culture models in drug discovery and drug repositioning. Front Pharmacol. 2018;9:6.
232. Fang Y, Eglen RM. Three-dimensional cell cultures in drug discovery and development. SLAS Discov. 2017;22(5):456–72.
233. Lee DW, Yi SH, Jeong SH, Ku B, Kim J, Lee M-Y. Plastic pillar inserts for three-dimensional (3D) cell cultures in 96-well plates. Sens Actuators B Chem. 2013;177:78–85.
234. Zeitlin BD, Dong Z, Nör JE. RAIN-Droplet: a novel 3D in vitro angiogenesis model. Lab Invest. 2012;92(7):988–98.
235. Mueller D, Kramer L, Hoffmann E, Klein S, Noor F. 3D organotypic HepaRG cultures as. Vitro (2014)
236. Thoma CR, Stroebel S, Rösch N, Calpe B, Krek W, Kelm JM. A high-throughput–compatible 3D microtissue co-culture system for phenotypic RNAi screening applications. J Biomol Screen. 2013;18(10):1330–7.

Publisher's Note